PATTERNS IN THIN LIQUID CRYSTAL FILMS AND THE DIVERGENCE ("SURFACELIKE") ELASTICITY

O. D. LAVRENTOVICH* AND V. M. PERGAMENSHCHIK*

Liquid Crystal Institute, Kent State University, Kent, Ohio 44242

Thin submicron and micron films of liquid crystals placed between two isotropic media represent a particular example of confined systems. Such films can be prepared on the surface of glycerin or other liquids. In comparison with Langmuir monolayers, these films are macroscopically thick to involve the liquid crystalline order in the interplay between molecular structure and macroscopic organization. At the same time, the films are thin enough for such a strong competition between surface and bulk properties that transitional in-plane symmetry is spontaneously violated and a number of patterns appear: stripe domains, square lattices, strings, high strength defects and so on. We show that these structures are governed by the divergence (or "sufacelike") K_{13} and K_{24} terms in the nematic free energy which have been ignored for decades. We also show that both terms can be included in the standard elasiticty theory without contradictions with the basic idea of the nematic phase. The one-dimensional confinement makes the films a unique object of investigation: although the phenomena observed are attributed to the vertical confinement, their manifestation is detected in a non-restricted film plane.

1. Introduction

Thermotropic liquid crystal films placed between two different isotropic media (e.g. nematic film with free surface spread on a glycerin of water) represent an example of confined systems. The Langmuir trough is the most convenient instrument to prepare and modify these films. We will use the abbreviation LLC (Langmuir Liquid Crystal) for such liquid crystal films. The LLCs are related to the following popular "soft matter" systems:

I. *Spreading isotropic liquid films* are presently under study in order to comprehend wetting and related phenomena.[1,2] The macroscopic and microscopic parts of the spreading liquid films are controlled by different laws resulting in a nontrivial film profile.

II. *Freely suspended liquid crystal films* provided rich infromation about surface interactions and effects of a reduced dimensionality on phase transitions and ordering over the last decade.[3-9] The studies have been carried out for smectic films freely suspended in air. Little is known about nematic free films which are hard to create and stabilize.[10,11] Nevertheless, an astonishing phenomenon of the deformed ground state is described for these films.[11]

---

*Also with the Institute of Physics, Ukraininan Academy of Sciences, Kyyiv, Ukraine.

III. *Langmuir monolayers of surfactant molecules anchored at an air/water interface.*[12-14] As number of new phenomena results from an intriguing influence of the microscopic properties (molecular structure, chirality, electric dipole moments of surfactant molecules, concentration of ions in the subphase) on macroscopic patterns.[12,13] The Langmuir monolayers can be classified using the nomenclature of smectic liquid crystals.[12] However, in monolayers there is no adjacent layer to couple to Ref. 14 and, consequently, there is no interplay between the surface and bulk forces.

IV. *Usual liquid-crystal cells.*[15,16] A rigid plate restricts director deformations in a cell because the anchoring forces keep molecules oriented along some preferred axis in both azimuthal and polar directions. It is hard to investigate the effect of low dimensionality using these cells because the thickness of the cells is typically larger than 1 μm.

V. *Confined liquid crystals* in the form of dispersed microdroplets, thin capillaries and porous media filled with liquid crystals represent rather new fields of research activites. A variety of new phenomena caused by the confined geometry has been observed recently.[17-27] In particular, the studies have provided a strong evidence that the surfacelike K_{24} elastic term cannot be ignored in the nematic free energy.[21-24]

Current research on systems I–V represents a scientific boom. The LLC's are expected to exhibit even more interesting behavior because of the following reasons.

(i) In comparison with spread isotropic liquid films, the LLC films have orientational ordering which is coupled to the flow and thus modifies wetting behavior.[28,29]

(ii) In contrast to films freely suspended in air, the LLC films are in contact with two *different* media. Therefore, the molecules have *different polar orientation* at the two interfaces, for example, perpendicular at the upper surface and tangential at the lower one. This hybrid alignment results in vertical deformations of the director field [30,31] (Fig. 1). An unexpected consequence of such a geometry is an appearance of states with periodic and non-periodic horizontal deformations and with broken chiral symmetry (even when the LLC film is composed of a simplest non-chiral nematic phase).[32-46]

(iii) The Langmuir monolayers are too thin to exhibit elasticity in the direction normal to the film plane. The LLCs possess an additional "elastic"degree of freedom: they are thick enough (10^2–10^4 moecules) to demonstrate the role of intrinsic liquid crystal ordering in the interplay between the molecular structure and macroscopic organization. Note also that the LLC surface can produce a symmetry breaking caused by molecular dipoles[47]; a similar effect is well-known for Langmuir monolayers. However, there is another remarkable possibility of the polar symmetry breaking in the LLC: director deformations in the vertical plane lead to so-called flexoelectric polarization[15] which is analogous to the piezoelectric effect in solids.

(iv) In contrast to usual liquid crystal cells, equilibrium states of LLC are not masked by azimuthal anchoring. Furthermore, the LLC films can be made thin enough ($\sim 1\,\mu$m and thinner) for the surface and bulk properties to compete (the ratio of the bulk elastic constant K to the surface anchoring coefficient W is typically $\sim 1\,\mu$m). Consequently, LLC's might demonstrate the role of such delicate mechanisms as splay canceling[30,36] and divergence elasticity[35,39,43–46] in pattern formation. In addition, there is a coupling between the director distribution and the film profile.[42]

(v) The LLC films are very different from other confined liquid crystalline systems such as suspended droplets or porous heterostructures because of the one-dimensional character of confinement. The phenomena caused by the confinement in one direction manifest as patterns in other two unrestricted dimensions. Therefore, these objects are relatively easy to study by means of optical methods.

Liquid crystal films placed on the isotropic substrate reveal many interesting properties connected with the peculiarities mentioned above: small (micron and submicron) thickness, difference in polar orientation at the two surfaces and absence of azimuthal anchoring. The most striking effect is the appearance of different patterns with horizontal deformations of the director field. The purpose of this review is to describe basic patterns formed in the LLC films and their connection with the problem of the divergence terms in the free energy. Note that we will operate with the free-energy functional derived for *three-dimensional* systems rather than with the two-dimensional version often used in the theory of Langmuir monolayers. In some cases the underlying physics can be illustrated equally in both two- and three-dimensional approaches. In fact, both Langmuir Liquid Crystals and Langmuir Monolayers show a number of similar patterns, such as stripe domain phase.
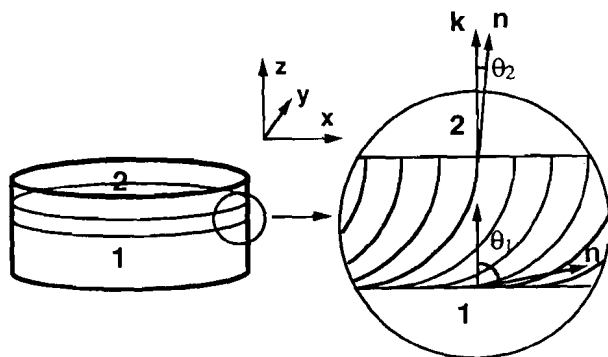

Fig. 1. Nematic film placed between two isotropic media "1" and "2". The media "1" and "2" generally impose different polar surface orientation of the director **n** (angles θ_1 and θ_2, respectively). As a result, **n** is distorted in the vertical plane. The azimuthal (in-plane) orientation of **n** is not fixed because of the isotropic nature of "1" and "2". The normal to the film surface is denoted **k**.

However, a complete description of the LLC films which includes both bulk elasticity and finite surface anchoring requires the general three-dimensional approach.

2. Basic Properties of the Hybrid Aligned Films

The experimental situation we are referring to is a film of thermotropic liquid crystal placed onto an isotropic substrate of different chemical nature, Fig. 1. In principle, the isotropic substrate can be the melted phase of the liquid crystal itself.[48-51] However, these biphasic systems are rather hard to investigate, since one has to create a temperature gradient. As a result, it is difficult to fix and measure the thickness of the liquid crystal film or to use temperature as a control parameter. Another problem is that the director distrotions in the film can affect the shape of the surface itself[15,52] because both the interfacial tension and difference in density of the two phases are relatively small.

   The LLC films floating on isotropic substrates of a different chemical nature are easier to investigate than biphasic systems. The temperature gradient is absent, and the parameters of the films can be controlled. Furthermore, the surface tension σ at the liquid crystal–isotropic fluid and liquid crystal–air interfaces ($\sim 10^{-2}$ J/m^2)[53] is usually a few orders of magnitude higher than the nematic-isotropic interface tension (reported[54] to be 10^{-4}–10^{-5} J/m^2). High σ magnitude together with typically large difference in density of the liquid crystal and the isotropic fluid substrate ($\sim 2 \times 10^2$ kg/m^3 for 5CB - glycerin system) decrease the interplay between the *isotropic part* of the surface energy and the elastic forces.

   There are three crucial features of the LLC films that make their properties unique:

(1) The polar tilt angles θ_1 and θ_2 of the director n at the two surfaces are generally different, since the two ambient media are different. This difference acts as a source of director deformations in the vertical direction. A nematic film with different polar orientation of n at the upper and lower interfaces is called a hybrid aligned nematic (HAN) film.

(2) Because of the isotropic nature of the ambient media, the molecular interactions at the both interfaces do not determine the azimuthal orientation of a liquid crystal. In other words, the azimuthal anchoring energy is zero, and the director configurations can rotate in the film plane without any energy cost. Since the boundary conditions are azimuthally degenerate in the film plane, it is relevant to denote a nematic LLC film as a HAND film, where D indicates such a degeneration.

(3) The thickness of the film is comparable with or smaller than the de Gennes–Kléman anchoring length $l = K/W$. Here, $W \sim (10^{-7} - 10^{-4}J/m^2)$[55] is the anchoring coefficient which characterizes the work needed to deviate the director from its equilibrium orientation at the surface. To illustrate the concept of the anchoring coefficient, imagine a surface that provides a normal orientation of n. The minimal value of the surface free energy $\sigma(\theta)$ is $\sigma_\perp = \sigma(\theta = 0)$. Any

changes in the tilt angle increase the surface energy. If the function $\sigma(\theta)$ is monotonous, then the maixmum $\sigma_\parallel = \sigma(\theta = \pi/2)$ will be reached at $\theta = \pi/2$. The anchoring coefficient W can be defined as the difference $\sigma_\parallel - \sigma_\perp$. The anisotropic part of the nematic surface energy is usually much smaller than the isotropic part, i.e. $W \ll \sigma_\parallel, \sigma_\perp$. Typical values of the elastic constant $K \sim 10^{-11}$ N give $l \sim 0.1\text{–}100$ μm. Consequently, the balance of the surface anchoring and bulk elasticity is of prime importance for the LLCs. Moreover, as we shall see, pattern formation in LLCs films is strongly influenced by the divergence elasticity.

The first LLC-like samples were prepared on a water substrate by Press and Arrott[30] and by Proust, Perez and Terminassian–Saraga[31] twenty years ago. These pioneering studies focused on the balance of bulk elasticity and surface anchoring[31] and on the properties of usual point defects with strength $m = 1$. Later studies[32–46] have revealed many interesting structures in the LLCs that do not occur in other soft matter objects. The microphotographs in this review represent the polarizing-microscope textures observed in thin nematic and smectic A LLC films. In most cases a glycerin substrate is used. External fields as well as temperature gradients are absent. The textures reveal many striking features, such as defects with high strength $m| > 1$,[36] strings,[33] and different periodic domain patterns.[34,35] The ability to form periodic spactial structures either due to specific molecular interactions (cholesteric, smectic, and blue phases) or under the influence of electric or magnetic fields is one of the most important and well-known properties of liquid crystals. In the present case, however, one deals with translationally symmetric (nematic) phase under no external field action.

Despite the absence of external fields or temperature gradients, the sophisticated patterns in LLCs are not without a special reason. Evidently the cause is the balance of the elastic forces and surface interactions. Full description of the patterns is not a simple problem since both elastic and surface properties of liquid crystals are surprisingly far from being completely understood. One of the controversial issues is the so-called "surfacelike elasticity", represented in the free elastic energy by the divergence terms.

3. Frank–Oseen Free Energy: the Pure "Bulk" and "Suracelike" K_{24} and K_{13} Terms

The standard situation in the field theories of elementary particles and condensed matter is that the free energy terms which have the form of a total divergence can be omitted. Liquid crystals present a unique situation where divergence terms (often called "surfacelike" terms) are, in fact, meaningful. Although these terms, called K_{13} and K_{24} terms, are derived on the equal basis with all other terms of principal order, for about fifty years they have been disregarded. Inclusion of these terms in the elasticity theory seemed to be even more murky than the reasoning to disregard

them and the problem of divergence terms has been a fundamental puzzle in the macroscopic physics of liquid crystals.

The conventional free elastic energy functional quadratic in the director derivatives can be written as

$$F_2 = \int dV \{ f_{\mathrm{F}} - K_{24} \nabla \cdot [\mathbf{n}(\nabla \cdot \mathbf{n}) + n \times (\nabla \times \mathbf{n})] + K_{13} \nabla \cdot [\mathbf{n}(\nabla \cdot \mathbf{n})] \} , \quad (1)$$

where

$$f_{\mathrm{F}} = \frac{1}{2} K_{11} (\nabla \cdot \mathbf{n})^2 + \frac{1}{2} K_{22} (\mathbf{n} \cdot (\nabla \times \mathbf{n}))^2 + \frac{1}{2} K_{33} (\mathbf{n} \times (\nabla \times \mathbf{n}))^2 . \quad (2)$$

The coefficients are called splay (K_{11}), twist (K_{22}), bend (K_{33}), mixed splay-bend (K_{13}), and saddle-splay (K_{24}) elastic constants.

The divergence K_{13} and K_{24} terms can be converted to surface integrals by the use of Gauss's theorem so that F_2 becomes

$$F_2 = \int dV f_{\mathrm{F}} + \int dS (f_{24} + f_{13}) , \quad (3)$$

where

$$f_{24} = -K_{24} \mathbf{k} [\mathbf{n}(\nabla \cdot \mathbf{n}) + \mathbf{n} \times (\nabla \times \mathbf{n})] , \quad (4)$$

$$f_{13} = K_{13}(\mathbf{kn})(\nabla \cdot \mathbf{n}) , \quad (5)$$

and $\mathbf{k}$ is a unit vector of external normal to the surface S of the sample.

Owing to Eq. (3), the divergence terms are often called "surfacelike" in spite of the entirely common nature of all the five elastic terms: all the five represent specific fractions of the bulk free energy density. Moreover, as we shall see, the pure "bulk" terms f_F also contain a "surfacelike" contribution. For this reason, keeping the word "surfacelike" in quotes would be most appropriate.

The f_{24} and f_{13} terms were introduced firts by Oseen[56] and Zocher[57]; they were subsequently abolished by Frank[58], and were then reinstated by Nehring and Saupe.[59] Although similar terms have also been explicitly introduced for superfluid ^{3}He [60,61] and can be introduced for ferromagnets,[62] they have been essentially ignored.

The standard reasoning for such an ignoring is borrowed from field theories[63] similar to the one-constant version of the elastic theory of the nematic phase. Namely, all the terms in Eq. (2) (taken with equal coefficients) are allowed by the symmetry for arbitrary vector field $\mathbf{n}$, and therefore the free energy of such a vector field can be written in the form $(\nabla \cdot \mathbf{n})^2 + (\nabla \times \mathbf{n})^2$. However, usually the field $\mathbf{n}$ is assumed to rapidly decrease towards the infinitely removed surface so that all divergence contributions are negligible. Then, by making use of the identity

$$(\nabla \cdot \mathbf{n})^2 + (\nabla \times \mathbf{n})^2 \equiv \sum_{i,j=1}^{3} (\partial_i n_j)(\partial_i n_j) + \nabla \cdot [\mathbf{n}(\cdot \mathbf{n}) + \mathbf{n} \times (\nabla \times \mathbf{n})] \quad (6)$$

the divergence term is separated from the total functional, and only the first term is retained, which is a pure bulk term.

Liquid crystal systems, in contrast, have actual surfaces whose specific shape and properties are known to be important. The disregard of divergence terms cannot be justified unless material parameters K_{13} and K_{24} vanish. There is, on the other hand, no fundamental reason why K_{13} and K_{24} should vanish or be negligible. Indeed, several different microscopic calculations have yielded for K_{13} and K_{24} the values of the same order of magnitude as for the standard Frank constants.[64-66] At the macroscopic level, it is easy to show that the status of the "surfacelike" constants is similar to those of the Frank constants. A good illustration of that is the radial director distribution in a spherical nematic droplet (so-called hedgehog) which is given by $n = r/r$ in the spherical coordinates (more complicated textures in droplets have been considered numerically[67,68]). The free energy of this radial "hedgehog" is

$$F_{\text{h}} = 4\pi R[K_{11} + (K_{11} - 2K_{24}) + 2K_{13}]. \tag{7}$$

Only the first term in Eq. (7) is a contribution of the "pure bulk" splay term in the right hand side of Eq. (6). The second term $(K_{11} - 2K_{24})$ is the total contribution of the terms that functionally coincide with the K_{24} term. Its K_{11} fraction is hidden in the Frank sum f_{F}, and only the $2K_{24}$ fraction corresponds to what is usually supposed to be the K_{24} term itself. Equation (7) clearly shows that the "surfacelike" and "bulk" terms are equally important even in geometries with a small surface/volume ration, i.e. when $R \to \infty$.

The contribution of the divergence terms strongly depends on the geometry of deformations. For example, the K_{24} term is always nonzero for topologically stable point defects such as hedgehogs,[21] boojums[36,39] or focal conic domains[69,70] but vanishes for the cylindrical radial distribution.[21] Generally, if n depends only on one Cartesian coordinate, the K_{24} term vanishes identically. At the same time, the K_{13} term never identically vanishes and might contribute in any geomtery. Thus, smallness or nonsmallness of the contribution to the free energy has nothing to do with a divergence character of the term, but it is defined by the value of corresponding elastic constant and the specific geometry of a problem.

An essential difference between f_{F} and divergence terms exists however. The matter is that f_{F} is positive definite whereas both the K_{24} and K_{13} terms are not. Therefore, the K_{24} and K_{13} terms can cause spontaneous deformations. This ability of the divergence terms is strongly enhanced in geometries with topological defects or with strong elastic deformations. We shall see that in thin HAND films these terms can cause spontaneous deformations violating parity, transitional and chiral symmetry.

Until recently there was a considerable doubt that the surfacelike terms could be introduced without any paradoxes. The present situation is that the K_{24} term is shown to give rise to no ambiguity.[71-73] There are several experimental estimations of K_{24} for nematic liquid crystals[21-24,39,46] ($|K_{24}| \sim K$) as well as of the correspond-

ing constant $\bar{K}$ in lamellar smectic phases.[69,70] We shall consider effects associated with K_{24} term in Sec. 5

The problem of the K_{13} term has required much more theoretical effort. Very recently, it was shown that the K_{13} term can be included in the standard elasticity theory without contradiction with the basic ideas of the nematic phase. [73] We shall consider this problem in Sec. 9.

4. The Homogeneous State of a Hybrid Aligned Nematic Layer

Let us consider a nematic layer parallel to the (x, y) plane and normal to the z-axis (Fig. 1). The lower $z = 0$ ("1") and the upper $z = h$ ("2") surfaces impose, respectively, tangential and normal (perpendicular) orientations degenerated in the (x, y) plane. Such a layer is what we call a HAND film.

We shall use the standard parameterization of the director

$$\mathbf{n} = (\sin\theta\cos\varphi, \sin\theta\sin\varphi, \cos\theta), \qquad (8)$$

where θ is the angle between $\mathbf{n}$ and the z-axis, $\varphi = \arctan(n_y/n_x)$. For a sufficiently thick HAND film, only the homogeneous state is realized. In a homogeneous state deformations are restricted to the vertical plane (x, z) and depend on a single variable z : $\theta = \theta(z), \varphi = 0$; therefore, $f_{24} \equiv 0$. If anchoring is stronger on the tangentially orienting surface S_1 i.e. $W_1 > W_2$, and the films is thinner than[74]

$$h_a = K_{11}(1/W_2 - 1/W_1), \qquad (9)$$

then $\mathbf{n}$ is undistrubed in the veritcal plane: $\theta(z) = \pi/2$. Here and henceforth we use the Rapini–Papoular anchoring potential, $W(\theta - \bar{\theta}) = \frac{1}{2}W_s\sin^2(\theta - \bar{\theta}_s)$, where $s = 1, 2$ and $\bar{\theta} = \frac{\pi}{2}, \bar{\theta}_2 = 0$.

In the approximation $K_{11} = K_{33} = K$, which will be used henceforth, the homogeneous state of HAND film is completely determined by the formula

$$\theta(z) = -\alpha z + \theta_1, \qquad \varphi = 0, \qquad (10)$$

where $\alpha = (\theta_1 - \theta_2)/h$. The boundary values θ_2 and θ_1 of the angle θ can be found from the equations

$$2(\theta_2 - \theta_1) + h(W_2/K)\sin 2\theta_2 = 0, \qquad (11)$$

$$2(\theta_2 - \theta_1) + h(W_1/K)\sin 2\theta_1 = 0, \qquad (12)$$

For a sufficiently thin HAND film, the homogeneous state (10) becomes ustable with respect to various perturbations $\delta\theta = \psi$ and φ when the free energy of the perturbed state $F_{\psi,\varphi}$ is lower than the energy of the homogeneous state F_{HS}. The critical condition for the transition is $F_{\text{HS}} - F_{\psi,\varphi} = 0$. We shall describe different

forms and mechanisms for nonzero ψ and φ to occur in thin HAND films. In what follows we shall use the notations $t = K_{22}/K$ and $p = 2K_{24}/K$.

5. Patterns and the K_{24} Elastic Term

5.1. *K_{24} mechanism of symmetry breaking in the absence of twist deformations*

How can the nematic layer with vertical curvature of n and zero aximuthal anchoring (Fig. 1) gain the energy? Surprisingly, the total energy of distortions can be *reduced by additional deformations in the film plane*. This can be illustrated by the following example.[36,39,44]

Let us consider the situation where twist deformations are absent and n is perpendicular to a set of surfaces $\sum$'s (Fig. 2). Each point of the surface $\sum$ is characterized by two principal radii of curvature R_1 and R_2 that define the mean curvature $(1/R_1 + 1/R_2)$ and the Gaussian curvature $1/R_1 R_2$ of $\sum$. The signs of R_1 and R_2 depend on the orientation (parallel or antiparallel) of the vectors $\mathbf{R}_1$ and $\mathbf{R}_2$ with respect to the chosen normal to $\sum$. For example, a sphere and an ellipsoid have only points with $1/R_1 R_2 > 0$; in contrast, a hyperbolic paraboloid (saddle surface) has only points with $1/R_1 R_2 < 0$.

Using the mean and Gaussian curvatures, the splay and K_{24} terms can be reexpressed as[16]:

$$(\nabla \cdot \mathbf{n})^2 = (1/R_1 + 1/R_2)^2 = 1/R_1^2 + 1/R_2^2 + 2/R_1 R_2 \,, \tag{13}$$

$$\nabla \cdot [\mathbf{n}(\nabla \cdot \mathbf{n}) + \mathbf{n} \times (\nabla \times \mathbf{n})] = 2/R_1 R_2 \,. \tag{14}$$

The difference in the polar anchoring sets the non-zero value of one of the principal radii of curvature, say, R_1. The homogeneous HAND film (Fig. 2a) is characterized by finite R_1 and infinite R_2 (Fig. 2d). As a result, for the homogeneous HAND state the splay term is equal to $K_{11}/2R_1^2$, and the K_{24} term is zero.

In the states with horizontal dformations (Figs. 2b and c) both radii are finite (Figs. 2e and f). The splay contribution $1/2K_{11}(1/R_1 + 1/R_2)^2$ decreases when R_1 and R_2 are of opposite signs (so-called splay-canceling mechanism,[30] Figs. 2b and e. Furthermore, with finite R_1 and R_2 there is another source of the energy gain: the K_{24} term becomes nonzero and reduces the total energy when $(-K_{24}/R_1 R_2)$ is negative. In contrast to bulk elastic moduli, K_{24} can be either positive or negative. Thus, $K_{24} < 0$ favors deformations with $1/R_1 R_2 < 0$, while $K_{24} > 0$ favors $1/R_1 R_2 > 0$ (Fig. 2).

Equations (13) and (14) show that the term responsible for the splay-cancelling and the K_{24} term functionally coincide. Thus, although it is sometimes useful to consider the splay canceling and K_{24} mechanisms separately, these mechanisms, in fact, are of the same divergence nature. As a consequence, we shall see that the total contribution of the term $\nabla \cdot [\mathbf{n}(\nabla \cdot \mathbf{n}) + \mathbf{n} \times (\nabla \times \mathbf{n})]$ to the free energy is proportional to $(1 - p)$ rather than to $(-p)$.
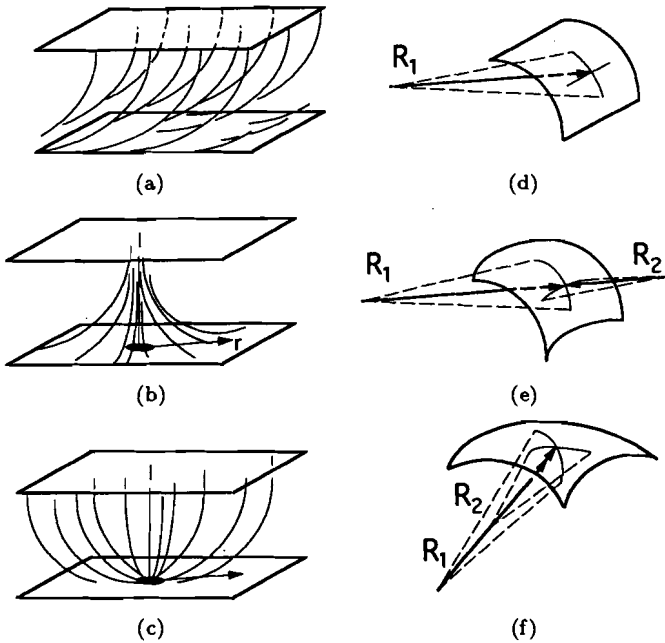
Fig. 2. Director distribution in a uniform HAND film (a) and in deformed states with $m = 1$ point surface defect (b.c). The Gaussian curvature $(R_1 R_2)^{-1}$ of the surfaces perpendicular to n is zero for the uniform HAND film (d), and nonzero negative (e) or positive (f) for the two defect states.

Qualitative consideration prompts that the states deformed both in the vertical and horizontal planes can be energetically preferable than the naively expected homogeneous state (10) because of non zero Gaussian curvature and zero azimuthal anchoring. These states can be used in a number of independent methods for determination of K_{24}. For example, K_{24} defines the film thickness threshold for periodic stripe domains.[35,46] The stripe domains behavior under the action of external field[43] or with thickness variations[45] also allows one to measure K_{24} (Sec. 5.4). Another approach is based on the peculiarities of strings[39] (Sec. 5.3).

5.2. *High strength defects*

5.2.1. *Low strength defects in conventional cells*

In thin flat nematic samples one observes textures with dark brushes. The brushes occur in areas where director n is parallel to either polarizer or analyzer of the microscope. Usually, defects possess the following properties;

1) The distribution of n around the defect is symmetrical. For example, if n is confined to the horizontal (x, y)-plane, then $n_x \sim \cos m\varphi$, $n_y \sim \sin m\varphi$. Here, m is the stength of the defect defined as the number of revolutions of n by multiples of 2π in going once around the defect core; $m = \pm 1/2, \pm 1, \ldots$.

2) There is a simple relation between m and the number N of dark brushes in the corresponding defect texture[75]:

$$|m| = N/4. \tag{15}$$

3) High-strength ($|m| > 1$) defects are prohibited. The higher m implies the greater curvature of n and, as a result, the greater elastic energy F. For the planar n,[16] $F \sim m^2$, and one observes only points with $N = 2$ or 4, i.e. $m = \pm 1/2$ and $m = \pm 1$. Rare cases of $N > 4$ textures have been observed in rather exotic nematic systems: lyotropic–theermotropic mixtures,[76] mixtures with special impurities,[77] and polymer nematic liquid crystals.[78]

4) Any defect with $m \neq 0$, as well as any nonuniform state with $m = 0$, costs an elastic energy which is greater than the energy of the uniform state (for the latter, $m = 0$ by definition).

Quite surprisingly, as we will see below, for the LLCs the above statements 1)–4) are false.[36,44]

5.2.2. *Textural observations for hybrid aligned films*

When observed under a polarizing microscope, LLC films with hybrid boundary conditions and thickness $1\,\mu\text{m} \leq d \leq 20\,\mu\text{m}$ exhibit rich arrays of point defects located at the lower surface of the film (favoring tangential orientation of n). From a topological point of view, these surface point defects are boojums[79] described first by Mermin for superfluid anisotropic liquid ^{3}He–A.[80] The main difference between boojums and bulk point defects (hedgehogs) is that the boojums cannot be moved away from the boundary.

Points with large $N > 4$ $N = 6, 8, 10, 16$ and sometimes even $N = 3, 5, 7$, etc.) are often observed in the HAND films, see Figs. 3 and 4, and Refs. 36 and 44. This is quite surprising, since $N > 4$ would normally mean that $|m| > 1$, see Eq. (15). The brushes are distributed nonuniformly: the angle ξ between two successive brushes is different for different sectros of the defect texture. There is a sector in the horizontal plane where $\xi \approx 90°$, and there are one or few sectors where ξ is much smaller ($\leq 10°$). Inside the first larger sector ($\Phi \leq \varphi \leq 2\pi$, sector I), the distribution is radial as for the $m = 1$ defect (Figs. 3a and 3b). The scarcity of the director revolutions up to $m \neq 1$ is filled up in the remaining narrow sector ($0 \leq \varphi \leq \Phi$, sector II). Figs. 3b and 4b. The sectors with high director curvature gradually transforms into strings of constant width (Sec. 5.3) that go away from the defect center.

In the vicinity of the defect center, $n(x, y, z)$ may be approximated as

$$n_x = \sin\theta(z)\cos M\varphi(x,y), \quad n_y = \sin\theta(z)\sin M\varphi(x,y), \quad n_z = -\cos\theta(z); \tag{16}$$

here, $M = M_\text{I} = 1$ for sector I, and $M = M_\text{II} = 1 + 2\pi(m-1)/\Phi$ for sector II.

(a)   (b)

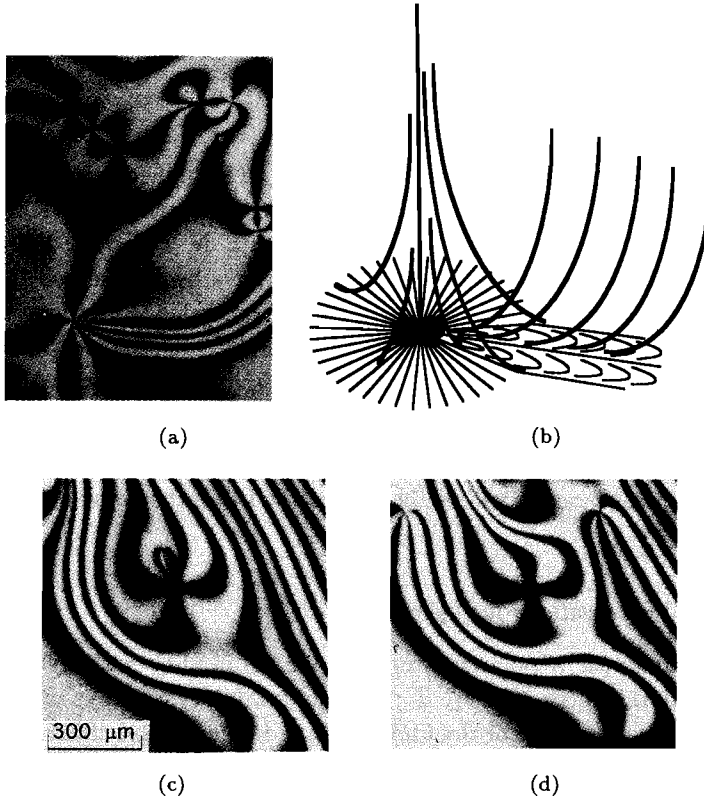(c)   (d)

Fig. 3.   Texture (a) and structure (b) of a high-strength defect with $m = 2$ in a HAND film of 5CB placed on the isotropic substrate of glycerin. Annihilation of the $m = 2$ and $m = -1$ defects (c) results in the $m = 1$ defect (d).

The existence of points with $N = 6$ (Fig. 4) or 10 brushes[36] (generally, $N = 4k + 2$, where k is integer) is especially surprising. In accordance with Eq. (15), these textures must correspond to half-integer strength defects, $|m| = k + 1/2$. On the other hand, half-integer defects are prohibited by the polar symmetry of the HAND film. Indeed, for the horizontal projection $\mathbf{n}_{xy}$ of the director field one has $\mathbf{n}_{xy} \neq -\mathbf{n}_{xy}$, and the point defect with half-integer $|m|$ should contain a singular line where two regions with opposite directions of $\mathbf{n}_{xy}$ met.

The paradox with nontrivial N is caused by the fact that Eq. (15) is not valid in the general case. Equation (15) was derived under the assumption that the defect possesses a symmetrically deformed structure, which is not the case of defects in HAND films. For example, Fig. 4 illustrates a singularity with $N = 6$. However, it is $m = 0$ rather than the $m = \pm 3/2$ defect, because all brushes in Fig. 4 form loops, i.e. they start and end at the same point, and therefore the whole configuration is topologically equivalent to the uniform state. Before we continue the discussion of the defects we have to consider a correct way of finding m.
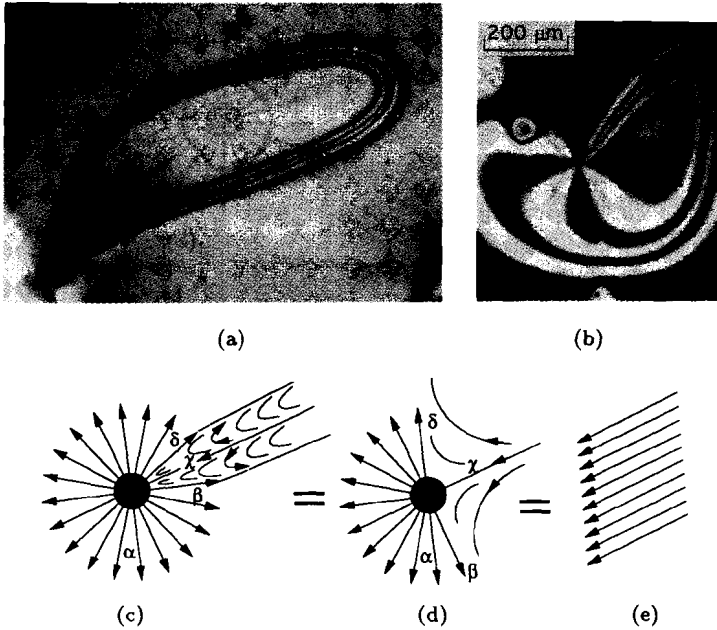
Fig. 4. Zero-strength defect $m = 0$ with 6 (a) and 8 dark brushes (b) that form loops; (c), (d), (e) the continuous transformation of the defect structure into the unifrom one in the vicinity of the defect core.

5.2.3. *Calculation of the defect strength*

The relation between $|m|$ and N can be found using a circle S^1 of unit radius that represents so-called degeneracy space for the in-plane vector field $\mathbf{n}_{xy}$.[20,79] Let us consider an example with a $m = 0$ defect, Fig. 5.

Each point of S^1 represents one particular orientation of $\mathbf{n}_{xy}$. The function $\mathbf{n}_{xy}(x, y)$ maps the points (x, y) of the real space into S^1. When one moves around the defect core along a closed loop $\alpha \beta \chi \delta$ (Fig. 5a), $\mathbf{n}_{xy}(x, y)$ draws a corresponding loop γ on S^1 (Fig. 5b). If the state is uniform, then γ is a point at S^1. If the state is nonuniform, but can be transformed into the uniform one (as shown in Fig. 4), then the loop can shrink into the point on S^1. If $\mathbf{n}_{xy}(x, y)$ has radial-like distribution with $m = 1$ (Figs. 2b and 2c), then γ coincides with S^1 since one meets all possible orientations of $\mathbf{n}_{xy}$ just once. For symmetrical defects $n_x \sim \cos m\varphi$, $n_y \sim \sin m\varphi$, each orientation of $\mathbf{n}_{xy}$ is realized exactly $|m|$ times; $|m|$ is an obvious topological invariant (strength) of the defect with sign defined by the orientation of γ.[20] In contrast, for non-symmetrical defects different $\mathbf{n}_{xy}$ orientations are realized a various number of times. For example, for the $m = 0$ defect some orientations of $\mathbf{n}_{xy}$ do not occur at all (those close to 2 o'clock), while all others appear twice (Fig. 5b).

Now, let us imagine that the structure is viewed through the microscope with polarizers, e.g. along the East–West (P, polarizer) and North–South (A, analyzer)
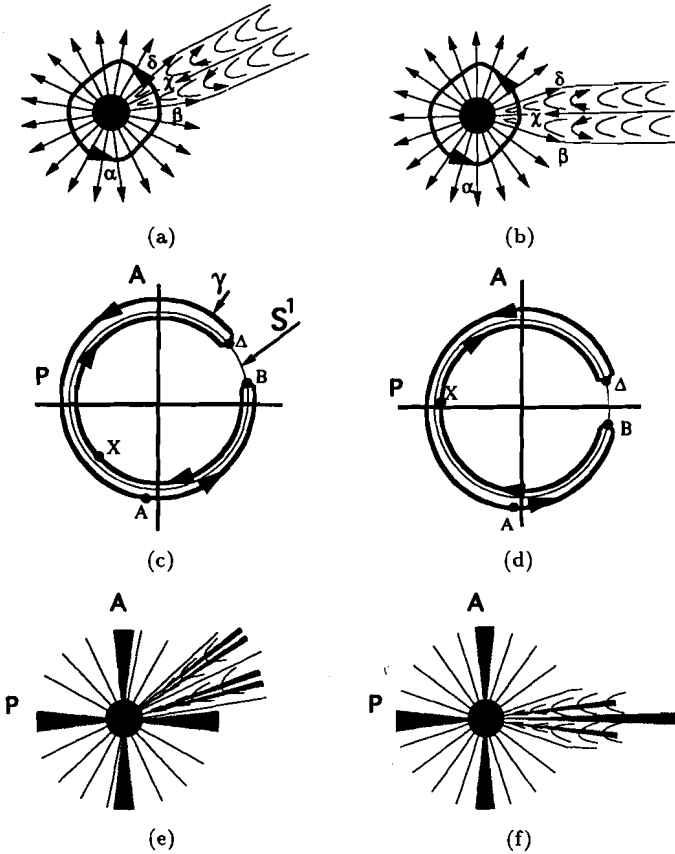
Fig. 5. Determination of the defect strength using the circle of the possible director orientations S^1: director distribution in the film plane (a, d); contour γ on the circle S^1 shows the orientation of the director around the defect (b, e); schematic textures of defects (a, d) viewing between the crossed polarizers of a microscope with 8 (c) and 6 (f) dark brushes; number of the brushes depends on the orientation of the defect structure with respect to the polarizers.

directions (Figs. 5b and c). The dark brush of extinction appears when n_{xy} is oriented along P or A; N is the number of times γ crosses lines A and P. Therefore, for the defect shown in Fig. 5a, $N = 8$ despite the fact that $m = 0$. It is important to note that N may be changed simply by sample rotation as shown in Figs. 5d, e and f: slight rotation of the structure between the crossed polarizers results in $N = 6$. As it is easy to see, any integer N (even such exotic as $N = 1, 3, 5, 7$, etc.) can correspond to the real defect configurations (including $m = 0$) in the hybgid aligned nematic LLC film. Therefore, Eq. (15) should not be used in the general case, and the strength of defects should be defined directly from the structure reconstructed by optical methods.[36]

5.2.4. *The elastic energy*

The nonsymmetrical structure of defects and the presence of the large sector I with radial structure play a crucial role not only in the textural peculiarities but also in the saving of the elastic energy.[36,39] To show this, it is sufficient to calculate the elastic energy F_1 of the defect with radial structure in the whole azimuthal plane ($m = 1$) and then compare this energy to the energy F_0 of the homogeneous state of the HAND film (Fig. 2).

In cylindrical coordinates (r, φ, z) the $m = 1$ defect distribution (Figs. 2b and e) is

$$n_r = \sin(\theta_1 - \alpha z), \quad n_\varphi = 0, \quad n_z = -\cos(\theta_1 - \alpha z). \tag{17}$$

Substitution of (17) into Eqs. (1) and (2) and integration over the range $r_c \leq r \leq R$, $0 \leq \varphi < 2\pi$, $0 \leq z \leq h$ yield

$$F_1^- = \frac{\pi K h}{2} \left[\alpha^2 R^2 + A \ln(R/r_c) - 2\alpha AR(1 - p)\right] + F_c^-, \tag{18}$$

where $A = 1 - \sin(\theta_1 - \theta_2)\cos(\theta_1 + \theta_2)/(\theta_1 - \theta_2)$, r_c is the radius of the defect core with energy $F_c \sim W_1 r_c^2 + K r_c$, and W_1 is the anchoring coefficient at the boundary with tangential orientation. The superscript "−" indicates that the defect under consideration has negative saddle-splay curvature (Figs. 2b and e).

On the other hand, the energy of the homogeneous HAND state is

$$F_0 = \pi K h \alpha^2 R^2 / 2. \tag{19}$$

The comparison of (18) and (19) shows that *the defect state may be energetically preferable than the uniform state* owing to the (i) splay canceling mechanism and (ii) saddle-splay mechanism that are represented by the two terms in Eq. (18), i.e. $(-2\alpha AR)$ and $(4\alpha ARK_{24}/K)$, respectively.

Splay canceling. The term $(-2\alpha AR)$ is obviously negative since both A and α are positive. With $K_{24} = 0\,K = 10^{-11}N$, $d \sim r_c \sim 10\ \mu$m, and $W_1 = 10^{-5}$ J/m^2, one obtains $F_1 < F_0$ if $R/d > 1$, i.e. the defect state is preferable than the uniform distribution of $\mathbf{n}_{xy}$. This result is a consequence of the principle of splay canceling[30,36]: if the boundary conditions force a variation of $\mathbf{n}$ in one direction, then a variation of $\mathbf{n}$ in another direction can lead to cancellation of the splay contribution. Splay canceling may be illustrated by rewriting $(\nabla \cdot \mathbf{n})^2$ as a function of the principal radii of curvature R_1 and R_2, (Eq. (13)). The elastic energy reduces when $R_1 R_2 < 0$. For the uniform HAND film, $R_1^{-1} \sim \alpha, R_2^{-1} = 0$, while for the defect state shown in Fig. 2b, $R_1^{-1} \sim \alpha, R_2^{-1} \sim r^{-1} \neq 0$, and $R_1 R_2 < 0$.

Saddle-splay mechanism.[39] The sign of the saddle-splay contribution might be either negative or positive as defined by the sign of the elastic constant K_{24} and the geometry of curvature. In the case of Figs. 2b and e, the defect energy will be decreased for $K_{24} < 0$. However, one may consider the opposite situation when the $m = 1$ defect has positive Gaussian curvature[39] (Figs. 2c and f)

$$n_r = \sin(\theta_1 - \alpha z), \quad n_\varphi = 0, \quad n_z = \cos(\theta_1 - \alpha z). \tag{20}$$

The saddle-splay contribution favors this defect if $K_{24} > 0$:

$$F_1^+ = \frac{\pi K h}{2}\left[\alpha^2 R^2 + A\ln(R/r_c) + 2\alpha A R(1-p)\right]F_c^+ ; \qquad (21)$$

there is no energy gain from the splay term.

Saddle-splay deformations save the elastic energy not only for $m = 1$ structures, but also for $|m| > 1$ and $m = 0$ configurations since these configurations contain broad sector I with $m = 1$. After insertion of (16) with $M_I = 1$ and $M_{II} = 1 + 2\pi(m-1)/\Phi$ into Eqs. (1) and (2), one obtains the elastic energy of the non-symmetric defect of strength m which contains the radial-like sector

$$F_m^\pm = F_{c,m}^\pm + \frac{\pi K h}{2}\left\{\alpha^2 R^2 + A\left[2m - 1 + 2\pi(m-1)^2/\Phi\right]\ln\left(\frac{R}{r_c}\right)\right.$$
$$\left. \pm 2\alpha A R\left(1 - \frac{\Phi}{2\pi}\right)(1-p)\right\}, \qquad (22)$$

where signs "$\pm$" indicate the type of the $m = 1$ sector.

The equilibrium value of Φ is obtained by minimizing $F_m^\pm$:

$$\Phi_0^\pm = \pi(m-1)\sqrt{\frac{2\ln(R/r_c)}{\mp\alpha R(1-p)}}. \qquad (23)$$

As a result, for sufficiently large R/h defects with $m \neq 1$ might be energetically more preferable than the state with uniform n_{xy}. For example, for a $m = 2$-defect with $\Phi_0 = \pi/2$, even with $K_{24} = 0$, one obtains $F_2 < F_0$ when the saddle-splay curvature is negative and $R/h > 6$.

5.3. *Strings and linear interaction between point defects*

There is an almost obvious structural similarity between topological defects in liquid crystals and elementary particles or defects in superfluids and ferromagnetics. Furthermore, liquid crystals offer the remarkable possibility of studying the dynamic aspects of singularities and the behavior of defects produced during a symmetry-breaking phase transition (see, e.g. Ref. 81). The particular boundary conditions of HAND films make it possible to observe qualitatively different regimes of the defect dynamics and interactions.[33]

The dynamics of point defects was studied in Ref. 33 for the HAND films with thickness ranging from 1 μm to 100 μm. The most interesting structural peculiarity of the films with thickness $\sim$(1–30) μm is that the nonuniform distribution of n between boojums of opposite topological charge is trectched out into a string with well-defined width D ($D = 100$–$300\,\mu$m, depending on the film thickness). Each string is seen in the polarized light as four parallel extinction brushes (Fig. 6).
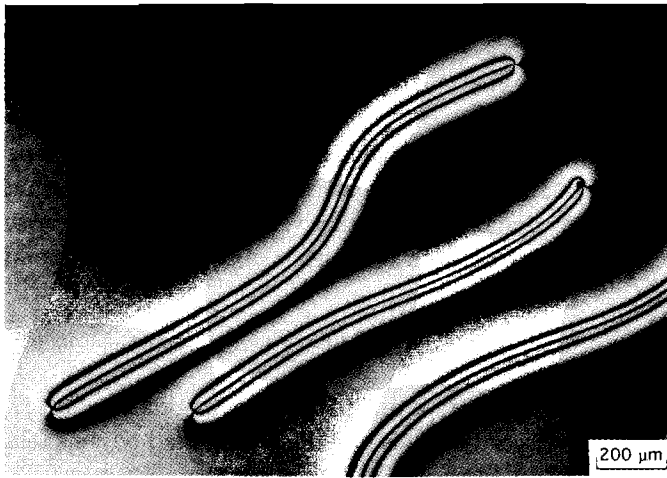
(a)
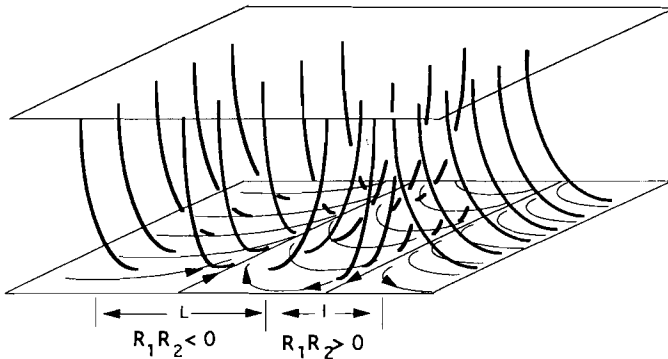
(b)

Fig. 6. Strings connecting point defects-boojums in a HAND film (5CB on glycerin, crossed polarizers) (a) and one of the possible director distributions (b).

The director n undergoes a 2π rotation within the string. Outside the string n is uniform in the horizontal plane. However, if the thickness of the LLC film is larger than $\sim 50\,\mu$m, the strings do not occur, and the director field between the pair of boojums expands in the horizontal plane.

As time elapses, the boojums close on each other and annihilate. As it has been found in Ref. 33, if the boojums are connected by a string the closing velocity v does not depend on the string length. Since the dynamics of the annihilation is defined by the elastic interaction of defects and by frictional forces, these data cast some light on the form of the interaction potential.

The width of the string is constant. Therefore, the elastic energy of the string is proportional to its length L. In other words, the interaction potential of the two

end point singularities depends linearly on L,

$$U(L) = aL\tilde{K}, \tag{24}$$

where a is a constant, and $\tilde{K} \sim K$ is a combination of the elastic constants.

The dynamics of a string is a dissipative motion of boojums which experience a frictional force proportional to the closing velocity v. Under the assumption that the friction acts identically on both boojums, the equation of motion is

$$\frac{\partial V}{\partial L} = F_{\text{friction}}, \tag{25}$$

where $F_{\text{friction}} = \gamma v D$ (the energy is dissipated in the region of width D), and γ is an effective orientational viscosity. Thus one finds that the boojums' closing velocity does not depend on L

$$v = aK/\gamma D = \text{const.}, \tag{26}$$

in agreement with the experiment. The linear nature of $L(t)$ manifests itself as a linear interaction between the defects, (Eq. (24)). The force of the interaction does not depend on the separation distance as in the case of quarks.

The dynamics of defects is completely different when the string confinement is absent. Experimentally, the string does not occur when the hybrid aligned film is thick ($h \geq 50\,\mu\text{m}$). The most probable reason is the two-dimensional character of the n field near the boundary with tangential orientation (where the boojums are located) for a thick sample. In the two-dimensional case, the interaction of the point singularities obeys the logarithmic law

$$U = 2\pi K h' \ln (L/D), \tag{27}$$

where h' is an effective thickness of the layer in which the tangential orientation is preserved. Using the equation of motion (25) and the definition $v = -dL/dt$, one finds that the annihilation time is proportional to the square of the distance between the defects, $\tau \sim L^2$, or, in other words,

$$L(t) = L_0 \left(1 - 4\pi K h't/\gamma L_0^2 D\right)^{1/2}, \tag{28}$$

where L_0 is the separation distance at the moment $t = 0$.

The very existence of the 2π-strings in thin HAND films and their absence in thick films remains an unsolved, intriguing problem. The appearance of strings can be related to the three-dimensional character of deformations in thin films (where n rapidly reorients from tangential to normal alignment along the veritcal axis). The string energy obviously contains the surface-like terms; this property can be to measure the corresponding constants. The string model with $K_{24} \neq 0$ and $K_{13} = 0$ was considered in Ref. 39.

As was already indicated, n undergoes a rotation through 2π within the string width D. The deformation of n depends on all three Cartesian coordinates and thus the saddle-splay elastic contribution to the string energy is nonzero. The important point is that there are two different π-turns within the width D that differ in sign of the saddle-splay contribution: one within width l and another within width L. Thus $l + L = D$, but as follows from the experiment, $l \neq L$ (Fig. 6). Employing director distribution with different in-plane curvatures for the l and L-substrings, one can see that the saddle-splay term contributes with different signs to the line tensions F_l and F_L of these two π-substrings[39]

$$F_l = \frac{K}{2}\left[\alpha_l^2 lh + \frac{\pi^2 hA_l}{2l} - 2\alpha_l hA_l(1-p)\right] + F_{\text{anch},l}\,, \tag{29}$$

$$F_L = \frac{K}{2}\left[\alpha_L^2 Lh + \frac{\pi^2 hA_L}{2L} + 2\alpha_L hA_L(1-p)\right] + F_{\text{anch},L}\,. \tag{30}$$

Here, $F_{\text{anch},L}$ and $F_{\text{anch},l}$ are the corresponding anchoring contributions.

The line tensions F_l and F_L of the two bands should be equal to each other because the string as a whole tends to be a straight line. Using this condition, an expression for the ratio K_{24}/K can be obtained that depends on the width of the substrings, film thickness and the anchoring energy.[39] Therefore, the measurements of the parameters of the strings can be used to estimate K_{24}/K. However, this method is restricted by the necessity of independent measurement of the polar anchoring strength.

## 5. K_{24} Mechanism of Spontaneous Twist Deformations and Stripe Domains

Stripe domains are the most regular and simplest patterns observed in the nematic LLC films of thickness $h \leq 1\,\mu\text{m}$.[35] The domain period L is a function of h. The dependence $L(h)$ can be obtained both experimentally and theoretically, which makes the stripe domains promising for studying the divergence elasticity. Although the stripe phase is attributed to a geometry with essentially submicron thickness, it is detected on supramicron scales (Fig. 7). Subsequently, the dimensionless wave number $\chi = 2\pi h/l \ll 1$. Smallness of χ enables one to develop the detailed theory of the phenomenon.[35,45]

The theory[35,45] implies the presence of all types of director deformations, including twist. In the absence of twist the term $1/(R_1R_2)$ in $(\nabla \cdot \text{n})^2$ functionally coincides with the K_{24} term (see Eqs. (13) and (14)). If, however, there are twist deformations, the representation in terms of normal surfaces $\sum$ and their curvatures is no longer possible. In this case, the K_{24}-like contribution can be separated from f_F by means of the general identity (6).

For the homogeneous hybrid state (10) to be unstable with respect to the perturbations $\delta\theta = \psi(y,z)$ and $\varphi(y,z)$ periodic along the y-axis (Fig. 7), the leading
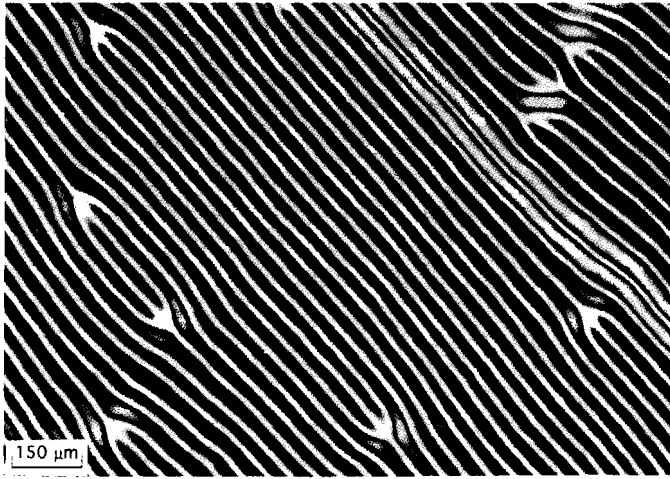
(a)
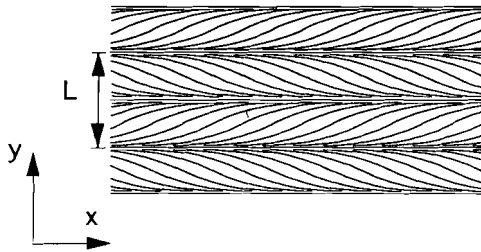
(b)

Fig. 7. Periodic stripe domains in thin nematic film ($h \approx 0.4$ μm, 5CB/glycerin) (a); schematic director structure in horizontal projection (b).

part $\delta^2 F$ of their energy, which is quadratic in ψ and φ, must be negative. After rather routine calculations we have

$$
\delta^2 F = \frac{K}{2L} \int_0^h dz \int_0^L dy \Big[\psi_z^2 + t\psi_y^2 + \sin^2 \theta \varphi_y^2 + \sin^2 \theta \Big(1 - (1-t)\sin^2 \theta \Big)
$$

$$
\times \varphi_z^2 - 2(1-t)\sin^2 \theta \varphi_z \psi_y \Big]
$$

$$
+ \frac{K}{2L} \sum_{s=1,2} \int_o^L dy \Big[2(1-p)(\sin^2 \theta \varphi \psi_y) + (W_s/K)\cos 2(\theta - \bar{\theta}_s) \Big] (z = z_s)
$$

$$
\tag{31}
$$

where the function $\theta(z)$ is given by Eq. (10) while its boundary values θ_1 and θ_2 are the h-dependent solutions of system (11), (12) (note that in previous Secs. 5.1–5.3, θ_1 and θ_2 were assumed to be h-independent for the sake of simplicity). There are only three terms in Eq. (31) that are not positive definite and can therefore result in a negative value of $\delta^2 F$. One of them is the surface term $\sim W_s/K$ which

corresponds to the well-known transition from the uniform state to the distorted homogeneous state $h = h_a$ (see Eq. (9)). This term is shown to be no way related to the periodic perturbations.[45] The second term is a bulk one of density $f_{22} = -2(1 - t) \sin^2 \theta \varphi_z \psi_y$. It is proportional to $1 - K_{22}/K$ and therefore the smaller K_{22}/K (typically, $0 < t \le 1$), the greater the absolute value of this term. Lastly, the third term is a surface term $f_{24} = 2(1 - p)[(\sin^2 \theta \varphi \psi_y)_2 - (\sin^2 \theta \varphi \psi_y)_1]$. It is proportional to $1-2K_{24}/K$, and its contribution grows with $|1 - p|$. It is natural to refer to the stability loss mechanisms, associated with the negativity of the f_{22} and f_{24} terms as to the K_{22} and K_{24} mechanisms, respectively. Both mechanisms are associated with the spontaneous violation of the chiral symmetry of n. In the homogeneous state both f_{22} and f_{24} vanish; their finiteness after the transition implies the existence of twist deformations.

The K_{22} mechanism of spontaneous twist deformations in nematic phase is well-known. Usually, K_{22} is smaller than K_{11} and K_{33}. If splay and bend deformations are sufficiently strong, their partial weakening by twist deformations is energetically profitable. The K_{22} mechanism is responsible for the formation of stripe domains in the Freédericksz transition when K_{22} is sufficiently small ($t \le 0.33$).[82] However, the situation is different in our case: stripe domains are observed in nematic liquid crystals with $t \sim 0.6$ and even with $t \sim 0.7$.[35] The matter is that $f_{22} \sim \chi^6$ whereas $f_{24} \sim \chi^4$, and hence for the long-wavelength stripe domains with $\chi \ll 1$ the K_{22} mechanism is merely not effective in comparison with K_{24} mechanism.[35,45] Thus, striped domains with $\chi \ll 1$ observed in Ref. 35 are driven by the K_{24} term. Particular cases of the appearance of the stripe domain phase were considered numerically in Refs. 38, 41, 43 and 46.

The most informative dependence describing the stripe domains in the nematic HAND films is the dependence $\chi(h)$ obtained in Ref. 45. We shall give more details about this in Sec. 9.7 after consideration of the K_{13} problem.

Note that the consideration given above does not take into account the possibility of smectic-like ordering near the interfaces, which is important for homeotropic alignment (Sec. 8). This approach is justified by the fact that the nematic films (0.1–1μm) are still much thicker than the possible smectic-like ordered regions ($< 0.01 \mu$m), and the orientation of molecules in the submicron region is almost tangential across the entire film thickness.

In contrast to the K_{22} mechanism, the K_{24} mechanism of chiral symmetry breaking is irrespective of the bulk constant anisotropy. Therefore, this mechanism might be important for other condensed media, such as superfluid ^{3}He and ferromagnetic phases.

6. Geometrical Anchoring

If a liquid crystal is in contact with an isotropic medium, the surface free energy depends only on the polar angle θ at the surface and is azimuthally independent. However, this statement is valid only in the particular case when the two surfaces of

the film are *parallel and flat*. In the general case of a nontrivial bounding surfaces, surface tilt leads to a well-defined azimuthal orientation which corresponds to the minimum of the free elastic energy.[42]

Let us consider a flat nematic film with degenerate tangential orientation on the upper surface and degenerate tilted orientation on the lower (Fig. 8a)

$$\theta(z = 0) = \theta_1 = \text{const.}, \quad 0 \leq \theta_1 \leq \pi/2. \tag{32}$$

Let us assume that the upper surface with tangential anchoring is inclined around the Y-axis (Fig. 8b). Now, $\theta(z = h)$ depends on the inclination angle γ and on the azimuthal parameter φ_0, which is the angle between $\mathbf{n}$ and the fixed axis X' in the inclined plane

$$\theta(z = h) = \arccos(\sin\gamma\cos\varphi_0). \tag{33}$$

The free-energy density in the absence of twist deformations

$$f = \frac{1}{2}K\theta_z^2 \tag{34}$$

leads the bulk equation

$$\theta_{zz} = 0. \tag{35}$$

The solution satisfying boundary conditions (32) and (33),

$$\theta(z) = \theta_1 + [\arccos(\sin\gamma\cos\varphi_0) - \theta_1]z/h, \tag{36}$$

gives a φ_0-dependent free energy per unit area (Fig. 8d),

$$\begin{aligned}
F &= F_0 + W_{\text{geom}} \\
&= \frac{K}{2h}(\Delta\bar{\theta})^2 + \frac{K}{2h}\left\{[\arcsin(\sin\gamma\cos\varphi_0)]^2 - 2\Delta\bar{\theta}\arcsin(\sin\gamma\cos\varphi_0)\right\}. \quad (37)
\end{aligned}$$

Here, $\Delta\bar{\theta} = \pi/2 - \theta_1$ is the difference in the polar anchoring at the two surfaces. The second term of Eq. (37) can be considered as the geometrical anchoring function W_{geom} with well-defined angular dependence.

The minimization of F with respect to φ_0 shows that the surface tilt imposes a preferred azimuthal orientation. If $0 < \gamma \leq \Delta\bar{\theta}$, the easy axis is aligned along the thickness gradient, $\varphi_{0,\text{eq}} = 0$ (Fig. 8b and d). With $\gamma = \text{const.}$ the increase of $\Delta\bar{\theta}$ leads to a sharper minimum in $F(\varphi_0)$. In the opposite case, $\gamma > \Delta\bar{\theta}$, one obtains nonzero solutions (Figs. 8c and d)

$$\varphi_{0,\text{eq}} = \pm\arccos(\sin\Delta\bar{\theta}/\sin\gamma). \tag{38}$$
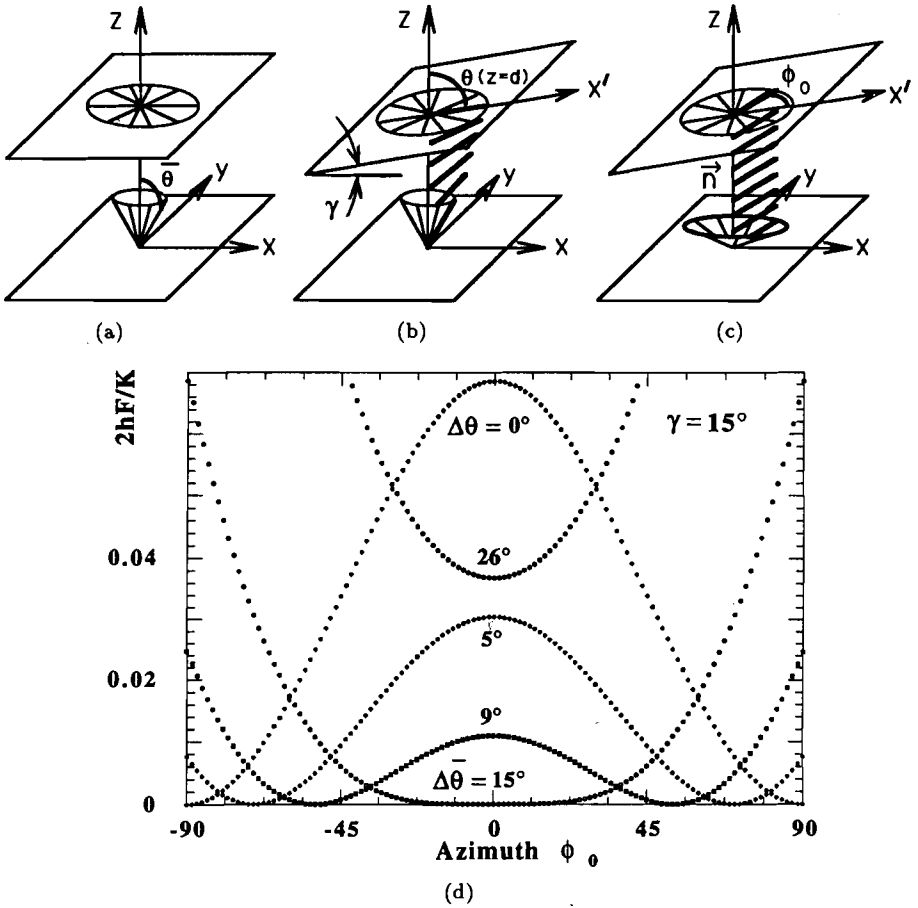
Fig. 8. The geometrical anchoring in a nematic film with non flat profile. a: Flat film with generally different polar anchoring. b, c: The surface tilt leads to the preferable orientation of n along $\varphi_{0,eq} = 0$, if $0 < \gamma \leq \Delta\bar{\theta}$ (b), and along nonzero $\varphi_{0,eq}$, if $\gamma > \Delta\bar{\theta}$ (c). d: The elastic energy of the film as a function of the azimuthal parameter φ_0. The upper surface is tilted by $\gamma = 15°$ with respect to the lower one. Different values of $\Delta\bar{\theta}$ are indicated in degrees units.

Any deviation from these "geometrical" easy axes will increase the free energy (Fig. 8d). This result is clear to understand. For example, if the lower plate sets the tangential orientation, $\theta_1 = \theta_2 = \pi/2$ and $\Delta\bar{\theta} = 0$, then n is absolutely uniform only for $\varphi_{0,eq} = \pm\pi/2$, and any other φ_0 would imply distortion.

One should distinguish the geometrical anchoring considered in Ref. 42 from de Gennes' coupling between the shape of the nematic–isotropic interface and the elastic distortions of the nematic bulk.[15,52] In accordance with Refs. 15, 52 the elastic energy of the nonuniform nematic can be reduced by the interface tilt if the interfacial tension and the density difference of the two media are sufficiently small. On the contrary, the geometrical anchoring does not imply the balance considered; the bulk distortions can be negligibly small and the interfacial tension

can be infinitely large. All that is needed is just the geometrical tilt of the surface, which can be induced by any factor including the interface tension.

The geometrical-anchoring approach can be applied to different geometries and media. Especially interesting consequences are expected for static configurations and dynamics of wetting LLC films. The spreading film typically has macroscopically thick and microscopically thin parts. There is an intermediate region where the film thickness rapidly varies and the surface tilt γ reaches some maximum value γ_{max} (e.g., see Ref. 83). The anchoring parameter $\Delta\bar{\theta}$ also changes along the film because of the finite polar anchoring. In other words, $\gamma/\Delta\bar{\theta}$ and the aziumthal orientations of $\mathbf{n}_{xy}$ vary along the normal to the film edge in accordance with Eqs. (37 and 38). These reorientations of $\mathbf{n}_{xy}$ give rise to domain walls that have been observed experimentally for non-flat nematic films placed on a glycerin surface.[42] Note that Jérôme and Boix[84] have observed periodic walls in the $\mathbf{n}_{xy}$ field that nematic films form on rigid substrates in the regime of oscillating surface tilt.

Another consequence of the geometrical anchoring is the optical activity in chemically non-chiral liquid crystal films or droplets when the sample is not flat and one of the surfaces sets physical azimuthal anchoring.[42] Let us imagine a tangentially achored nematic layer placed on a rubbed solid substrate. The rubbing sets unidirectional orientation $\varphi(z = 0) = 0$. The upper surface is free and also provides tangential anchoring which is, however, physically degenerate. If this surface is inclined, the geometrical anchoring tends to set $\varphi(z = h) = \pm\pi/2$. The balance between the physical and geometrical anchoring results in twist deformations that provide smooth reorientation of n from $\varphi(z = 0) \rightarrow 0$ at the lower rubbed plate to $\varphi(z = h) \rightarrow \pm\pi/2$ at the upper surface. Experimental data[85-87] indicate optical activity of the nematic droplets placed onto a rubbed or polished rigid plate. The discussed twist provides quite a natural explanation of this distracted phenomenon since the droplets have nonflat shape.[42]

7. Flexoelectricity

The flexoelectric effect in a nematic liquid crystal consists in the appearance of a macroscopic polarization $\mathbf{P}$ in regions with a nonuniform $\mathbf{n}$[15,88]

$$\mathbf{P} = e_1 \mathbf{n}(\nabla \cdot \mathbf{n}) + e_3(\nabla \times \mathbf{n}) \times \mathbf{n}. \tag{39}$$

e_1 and e_3 are the flexoelectric coeffiecients. Typically, the polarization is screened by ions. However, when the characterisitic size of the distorted region is sufficiently small as compared to the Debye screening length (e.g., in the case of small dispersed droplets), the screening is not so effective and consequences of the flexoelectric effect can be observed experimentally. One example is the possibility of ordering in systems of liquid crystal droplets.[88-91]

In the regime of incomplete wetting, a LLC film forms a convex lens-shaped droplet at the isotropic substrate. Each droplet contains a point defect because of the boundary conditions. Usually, the defect is located in the center of the droplet,[30]
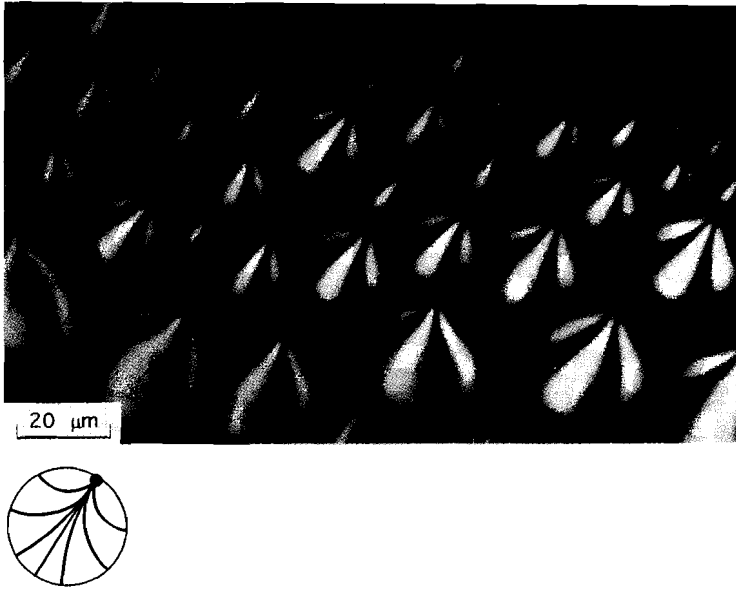
Fig. 9. Orientational ordering of the symmetry axes of lens-shaped nematic droplets (5CB) placed onto the polyisobuthylene substrate. Crossed polarizers. The scheme shows the director structure inside the droplet.

but in some systems it is shifted towards the periphery (Fig. 9). The broken symmetry gives rise to the dipole flexoelectric polarization along the horizontal axis. The interaction between the flexodipoles can lead to orientational ordering of droplets (as shown in Fig. 9).

Let us assume that a droplet has a cylindrical shape with a radius R and a height $h \ll R$. The boundary conditions are normal at the lateral surface and tangential at the upper and lower surfaces. The distribution close to that observed experimentally (Fig. 9) can be written in Cartesian coordinates as

$$(n_x, n_y, n_x) = [\cos 2\eta(x, y), \sin 2\eta(x, y), 0] , \tag{40}$$

where η is the angle between the radius vector $\mathbf{r}$ and the symmetry x-axis. The director distribution has a singularity at the origin of the coordinate frame which is placed on the edge of the droplet.

Using expressions (39) and (40) one finds the dipole moment of the droplet, $\mathbf{p} = \int_v \mathbf{P}dV$, which is directed along the symmetry axis x

$$\mathbf{p} = \pi(e_1 - e_3)Rh\hat{\mathbf{x}} . \tag{41}$$

To estimate the effectiveness of the dipole–dipole interaction of the droplets, we set $e_1 = -e_3$ and introduce the dimensionless constant $\lambda = p^2/a^3 k_{\mathrm{B}}T$, where a is the distance between droplets, T is the temperature, and k_{B} is the Boltzmann

constant. The ordered phase of dipoles forms when $\lambda \geq 60$[92] which corresponds to a distance $\sim 20\text{--}30\,\mu m$ between droplets.

It is pertinent to compare the interaction energy involved in the flexoelectric effect (e.g., the dipole–dipole energy $U_{pp} = p^2/a^3$) with the energy of the dispersive interaction of droplets[93,94] $U_{dd} \sim HR/12a$, where $H \sim 10^{-19}$ J is the Hamaker constant. For the parameters estimated above, $U_{pp}/U_{dd} < 1$ if $a \leq 700\,\mu m$. In other words, within the scales over which one would expect a coherent behavior of the droplets, the flexoelectric interaction can be predominant (if it is not screened by ions). It would be interesting to study this point in more detail experimentally.

8. Smectic Films

Smectic ordering can occur in LLC films even when the temperature of the sample is well above the smectic–nematic transition because the interfaces restrict the translation degree of freedom of the molecules. There are numeorous examples of the smectic A ordering at the free surface of the nematic and isotropic phases for normal boundary conditions.[55,95] Thin (less than 5 nm) translationally ordered regions occur even for tangential anchoring.[95] Below, we briefly discuss the LLC films composed entirely of a SmA phase. As in the case of nematic LLCs, the SmA film structure is strongly connected to the balance of surface and bulk forces.

The peculiarity of the elastic theory of SmA phase is that the twist and bend deformations are prohibited because these deformations violate constant interlayer separations. The normals $\mathbf{n}$ to the layers are everywhere straight lines and[96]

$$\mathbf{n} \cdot (\nabla \times \mathbf{n}) = 0, \quad \mathbf{n} \times (\nabla \times \mathbf{n}) = 0. \tag{42}$$

It is easy to see from Eqs. (42) and Eqs. (1)–(5) that not only the twist and bend terms do not enter the expression for the SmA elastic energy, but also the K_{13} and K_{24} terms cannot be separated from each other. Thus, one usually writes

$$F_{SmA} = \int dV \left[\frac{1}{2} K (1/R_1 + 1/R_2)^2 + \bar{K}/R_1 R_2 + \frac{1}{2} B \varepsilon^2 \right], \tag{43}$$

where R_1 and R_2 are the principal radii of curvature of the smectic layers, $\bar{K}$ is the saddle-splay elastic constant, and B is a compression modules that describes the elastic resistance to variations ε of the layer thickness d. Splay and compression elastic constants are related, $B = K\lambda^2$, where λ is a characteristic length ($\lambda \sim d \sim 30$ Å far from the thermotropic SmA–nematic phase transition).

The saddle-splay modules $\bar{K}$ has physical meaning similar to that of constant K_{24} in the nematic phase (note that the conventional signs of these two constants are opposite to each other, compare Eqs. (1), (14) and (43)). The vlaue of $\bar{K}$ for thermotropic SmA phase is unknown. There are few estimations of $\bar{K}$ for lyotropic SmA phases.[69,70] It turns out that for lyotropic SmA phase $|\bar{K}|$ can be even larger than K; besides, $\bar{K}$ adopts both positive and negative values depending upon the surfactant-to-cosurfactant concentration ratio.[70]

The energy densities carried by the system for pure curvature deformations ($\sim K/R^2$ or $\bar{K}/R^2$) or for a pure compression ($\sim B$) have very different magnitudes at large scales $R \gg \lambda$, which tells us that the SmA phase usually deforms in a set of equidistant and parallel surfaces without dilations.

(a)

(b)
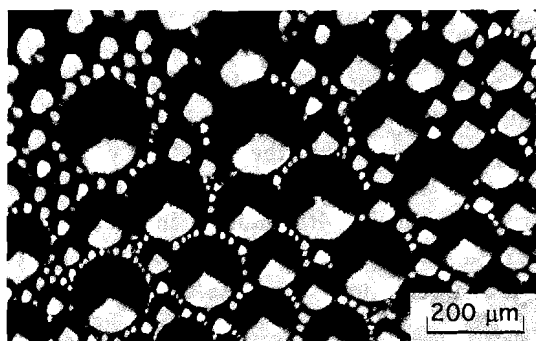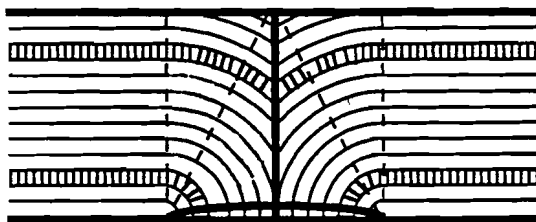
Fig. 10. The Appolonius packing of focal conic domains in smectic A film (8OCB/glycerin) (a); geometry of layers in the vertical cross section of the torical focal conic domain (b).

Let us suppose that the hybrid aligned nematic LLC is cooled to the SmA phase. The necessity to simultaneously satisfy hybrid boundary conditions and to maintain the layers' equidistance leads to the appearance of so-called focal conic defects (Fig. 10). Basic features of these objects are described in Refs. 15, 16 and 20. For a SmA LLC film one deals with the simplest case of torical domains (more complicated geometries might occur in a cell with rigid treated plates in the vicinity of the SmA-nematic transition[97]). The layers are folded around the circle which bounds the domain base and a straight line passing through the center of the circle (Fig. 10b). The region of deformations is restricted by the circular cylinder. It is remarkable that within the domain base the molecules are strictly tangential to the interface. Outside the domain, the molecules are normally anchored (Fig. 10). The evident reason for the domain appearance is the tendency of the substrate to orient molecules tangentially.

How do the torical focal conic domains with circular bases fill the LLC film? The most obvious solution is the Appolonius packing of circles on the plane.[16,96,98] One

begins with placing the largest possible domain with radius of the base $\sim h$. Then the remaining gaps are filled with smaller conical domains, etc. (Fig. 11a). The question is: what is the radius a^* of the smallest domain? If the filling is defined only by the bulk properties of the SmA phase, the smallest radius is of molecular size, $a^* \sim \lambda \sim \sqrt{K/B}$.[98] However, in reality the iterations are often interrupted at scales much larger than the moclecular size $(a^* \gg \lambda)$.[99] The reason is the anisotropy of the surface energy of the SmA phase.[99]

For a qualitative understanding it is sufficient to point out that there are two types of anchoring at the lower boundary (Fig. 10b): the normal one between the domains and the tangential one within the islands of domain bases. The surface energies $\sigma_\perp$ and $\sigma_\parallel$ for these two alignments are different. If $\Delta\sigma = \sigma_\parallel - \sigma_\perp < 0$, then the appearance of a small domain with radius a in between larger domains saves surface energy $\sim (-\Delta\sigma)a^2$, and the elastic energy cost is $\sim Ka$ (when $\bar{K} = 0$). The balance of the surface and curvature terms results in[99]

$$a^* \sim K/(-\Delta\sigma), \tag{44}$$

which can be very different from λ. For example, with $K \sim 10^{-11}$ N and $\Delta\sigma \sim -10^{-5}$ J/m^2 one obtains $a^* \sim 1\ \mu$m. On scales exceeding a^*, the space filling is realized by the Appolonius packing of domains; these domains provide the proper tangential surace alignment. On scales smaller than a^*, the remaining gaps cannot be filled with domains because the losses in elastic energy are larger than the surface energy gain. The described hierarchy is rather general for smectic textures[99]; for instance, it also governs the structure of so-called "bâtonnets" of the SmA phase emerging from the isotrpoic melt.[100] Critical radius (44) can be changed if $\bar{K} \neq 0$ (the energy of the focal conic domain contains linear combination of K and $\bar{K}$ terms[69]).

In the SmA phase the surface parameter $\Delta\sigma$ should not be mixed up with the anchoring coefficient W that describes the energetic cost of relatively small deviations from the equilibrium tangential or normal orientations. Only tangential and normal orientations at the surface are compatible with the SmA layered structure. Indeed, the tilt of layers at the boundary of an isotropic fluid implies either (1) the breaking of layers and preserving of surface flatness (if $\sigma \gg Bd$, Fig. 11a) or (2) rippling of the surface but preserving of the layer structure (if $\sigma \ll Bd$, Fig. 11b). The rippled interface can be described by a potential $\sigma(\theta) = \sigma_\parallel \sin\theta + \sigma_\perp \cos\theta (0 \leq \theta \leq \pi/2)$.

In the first case, W might be as high as 10^{-3}–10^{-2} J/m^2,[101] which is significantly higher than W usually measured for nematic liquid crystals. In the second case, the interface area increases by the factor $(\cos\theta + \sin\theta)^{-1} > 1$; consequently, $W \sim \sigma(\cos\theta + \sin\theta)^{-1}$ is comparable with σ. Usually $\sigma \gg |\Delta\sigma|$. For example, at the SmA–glycerin interface $\sigma \sim 10^{-2}$ J/m^2,[53] while $|\Delta\sigma| \sim 10^{-5}$ J/m^2.[99] Therefore, one can expect that $W \gg |\Delta\sigma|$ in both cases considered (note, that in the nematic phase $W \sim |\Delta\sigma|$). Large W can influence the focal conic domain patterns, since the SmA layers should be tilted at the surface containing the apex of the domain.[101]
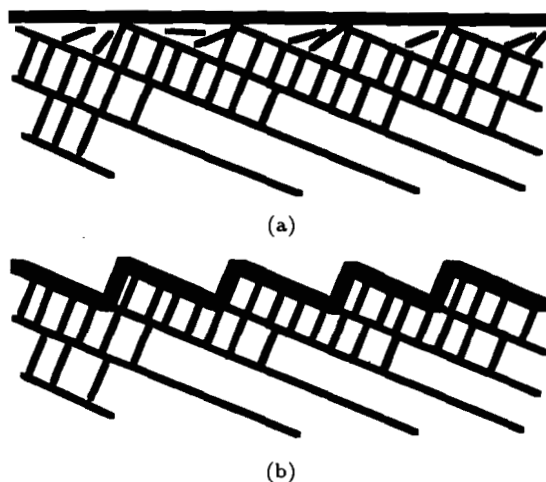
(a)

(b)

Fig. 11. SmA surface: the tilted orientation requires layer breaking (a) or interface rippling (b).

9. Inclusion of the K_{13} Term in the Standard Elasticity Theory

In the standard variational analysis, the surface contributions to functionals contain no derivative-dependent terms. An extremal family of functions for the standard functional satisfies the Euler–Lagrange equations. The problem is that the surface density of the K_{13} term is derivative-dependent and a minimizing procedure for the functional F_2 with $K_{13} \neq 0$, Eq. (1), is not known. In this respect, Oldano and Barbero[102] have made an important point that the K_{13} term leads to infinitely strong subsurface deformations; these deformations are a consequence of the fact that the K_{13} term is unbounded from below.[73,103] The paradox is that this result follows from the continuum theory where the deformations should be weak. Therefore, an interpretation of the K_{13} term must involve the resolution of the Oldano–Barbero paradox.

Rather than face this problem, Hinov[104–107] has postulated *a priori* that physical content should only be assigned to the Euler–Lagrange equations for the functional F_2. These equations, nevertheless, do not yield a minimum energy configuration.

On a different note, Barbero, Madhusudana and Oldano[65] have argued that to restrict the infinite deformations some fourth-order terms should be retained in the free-energy expansion. However, the predicted finite deformations are still very strong to be accommodated in a continuum theory where smooth variations over mesoscopic length scales are assumed.[15,56–59] Moreover, the question arises as to *which* fourth-order terms should be retained.

Derivative-dependent terms are also introduced in the expressions of the anchoring energy. Some surface energy densities quoted in the literature are

$$f_{\mathrm{RP}} = \frac{1}{2} W_{\mathrm{RP}} \sin^2(\theta - \bar{\theta}), \tag{45}$$

$$F_{\text{DVP}} = \frac{1}{2} W_{\text{DVP}} \sin[2(\theta - \bar{\theta})]\theta' , \tag{46}$$

$$f_{\text{M}} = \frac{1}{4} W_{\text{M}} \sin^2[2(\theta - \bar{\theta})]\theta'^2 , \tag{47}$$

referred to as Rapini–Popoular,[108] Dubois–Violette and Parodi,[89] and Mada[109] terms, respectively; here $\theta - \bar{\theta}$ is the angle between n and the easy axis e on S, and the prime denotes the derivative of θ along the normal k to S.

Another problem concerns the separation of the "surfacelike" elastic terms (which are just divergence bulk terms and depend exclusively on the properties of the nematic material) and the anchoring energy (which depends on the properties of both the surface and the nematic phase). Indeed, the anchoring term (46) has a structure similar (at least in the one-dimensional case) to f_{13}, Eq. (5). Formally this implies that the only observable quantity would be the sum elastic constant+relevant anchoring coefficient and the measured surfacelike elastic constants would be meaningful only in association with a pair nematic-surface. The question then arises as to whether a microscopic calculation, even formally unambiguous, would be of any use at all. However, even this microscopic unambiguity has been questioned.[11]

Thus, a consistent theory of the divergence elasticity must be able to answer the following questions[73]:

I.   *Is it possible to introduce the K_{13} term in the nematic free energy without any contradiction with the very idea of weak deformations?*

II. *Why, despite similarity between the K_{13} and K_{24} terms, only the K_{13} term causes difficulties, while the K_{24} term does not?*

III. *What is the role of the derivative-dependent terms in the anchoring energy?*

IV. *Is it possible to assign well-defined K_{13} and K_{24} values to a given nematic material?*

V.   *Are the constants K_{13} and K_{24} unambiguous quantities from the microscopic point of view[66]?*

First of all we shall formulate the mathematical essence of the problem.

9.1. Unboundedness of the Frank–Oseen functional form below for $K_{13} \neq 0$

Let us consider a nematic sample limited by two surfaces, $z = 0$ and $z = h$ (Fig. 1). In the one-dimensional case $\theta = \theta(z)$, the free energy of the sample, is

$$F_2 = \frac{1}{2} K \int_0^h \theta'^2 dz + W_1(\theta_1) + W_2(\theta_2) + \frac{1}{2} K_{13}(\theta'_1 \sin 2\theta_1 - \theta'_2 \sin 2\theta_2). \tag{48}$$

Standard procedure for finding $\theta(z)$ implies solving the Euler–Lagrange equation $\theta'' = 0$ with solution $\theta(z) = -\alpha z + \theta_1$. For this $\theta(z)$, functional (48) takes some

finite value which would have been its minimum in the standard situation. However, this value is not a minimum if $K_{13} \neq 0$. Indeed, let us choose $\theta(z) = bz^a + \theta_1$ in the vicinity of the surface $z = 0$; here, $1/2 < a < 1$ and b is an arbitrary constant such that $bK_{13} > 0$. For this $\theta(z)$, the K_{13} contribution becomes infinite negative

$$-K_{13}\theta_1' \sin 2\theta_1 \sim -K_{13}abz^{a-1} \sin 2\theta_1 \longrightarrow -\infty \,, \; z = 0 \,.$$

At the same time the bulk energy converges at $z = 0$,

$$K \int_0 \theta'^2 dz \sim a^2 b^2 z^{2a-1} \longrightarrow 0$$

so that $F_2 \rightarrow -\infty$. Therefore, the functional possesses no minimum at all unless K_{13} is strictly zero. The larger b the larger the drop in the free enrgy. On the other hand, n rotates through the angle $\Delta\theta \sim 1$ within the subsurface layer of thickness $\Delta z \sim b^{-a}$. Since b can be arbitrary large and hence Δz can be arbitrary small, such director deformation is merely a subsurface discontinuity. This fact has given rise to the idea that the nonzero K_{13} causes infinitely strong subsurface deformations.[102] Such a discontinuity is rather surprising result in the macroscopic theory because this theory presupposes that large deformation $\Delta\theta \sim 1$ occurs over distances much larger than the microscpic legth L_M. The discontinuity formally occurs not only in the flat geometry considered here but in arbitrarily shaped nematic samples.[73]

9.2. *Restriction of deformations and higher-order elasticity*

From the mathematical point of view, the unboundedeness of F_2 from below means that F_2 has no minimum. From the physical point of view, strong deformations contradict both the idea of the nematic phase and the assumption about the weakness of deformations underlying the derivation of the functional F_2. The mathematical inconsistency can be removed by adding to F_2 some terms R_h of order higher than that of F_2 in the operator ∂. The R_h terms bound the free energy from below, and hence ensure the existence of $\min(F_2 + R_h)$. For example, the authors of Ref. 65 propose the form $R_4 = \int P_4 (\partial^2 n)^2 dV$, where P_4 is some fourth-order elastic constant. Evidently, both the total free energy $F = F_2 + R_4$ and the director derivatives are now bounded. But to make the theory physically consistent is more difficult. Although the deformations become finite in this approach, their values are still too high, $L_M \partial n \sim 1$ on S, while in the nematic phase $L_M \partial n$ must be of the order $L_M/L \ll 1$, where L_M is a molecular length and L is the scale of deformations. It is clear that in the theory with $L_M \partial n \sim 1$ the scales L_M and L coincide; this makes a macroscopic description impossible.

    A further question arises as to whether one or several terms of fourth order must be introduced in R_4. Such an ambiguity could be removed by taking into account all possible terms of the fourth order in R_4. Although there are 35 such terms[59] with unknown elastic constants, even inclusion of them all does not solve the problem. Indeed, the total contribution of any order contains additional divergence terms,

which also are unbounded from below. For example, at order ∂^4 there is a term $\nabla \cdot (\mathbf{n}\Delta(\nabla \cdot \mathbf{n}))$, which introduces the third-order derivatives in the surface part of the free energy. Just as the K_{13} term is unbounded from below, this term removes the lower bound of the sum $F_2 + R_4$, which again has no minimum. Then, in order to restrict the $\nabla \cdot (\mathbf{n}\Delta (\nabla \cdot \mathbf{n}))$ term, one must take into account sixth-order terms, among which, however, the term $\nabla \cdot (\mathbf{n}\Delta\Delta(\nabla \cdot \mathbf{n}))$ exists, and so on. We see that it is impossible to solve the problem by introducing new elastic terms up to any finite orders.[73]

Moreover, let us for a moment assume that only the K_{13} term $\nabla \cdot [\mathbf{n}(\Delta)^0\nabla \cdot \mathbf{n}]$ survives, while an infinite number of similar terms $\nabla \cdot [\mathbf{n}(\Delta)^k\nabla \cdot \mathbf{n}]$ somehow disappear from the total energy expansion F for all $k > 0$. Then the restriction to the fourth order, i.e. $F \approx F_2 + F_4$, is meaningless itself. Indeed, $F_{2k} \sim (L_M\partial)^{2k}$,[15] and since the theory[65] predicts $(L_M\partial) \sim 1$, all F_{2k} are of the same order as F_2. Therefore, we again arrive at the necessity of considering the infinite series.

Thus, the K_{13} problem follows from two contradictory assertions:

(1) F_2 is unbounded from below for any $K_{13} \neq 0$;
(2) microscopic theories predict $K_{13} \neq 0$.[64-66] We shall show that there exists a unique solution of the problem within the framework of a consistent phenomenological approach.[73]

Such an approach must necessarily be consistent with the following ideas of the nematic phase:

(A) deformations are weak, $L_M|\partial n| \sim L_M/L \ll 1$;
(B) a satisfactory theory must employ only the functional F_2 quadratic in the operator $L_M\partial \sim L_M/L$.

This means that although the higher-order terms F_{2k} for $k = 2, 3, \ldots$ in principle can play an important mathematical role in the theory, they must not enter explicitly the observable quantities, i.e. $|F_2| \gg |R_\infty|$ where $R_\infty = \sum_{k=2}^{\infty} F_{2k}$. It is clear that (B) can be satisfied only due to (A) since it follows from (A) that $F_{2k} \sim (L_M/L)^{2k}$.[59] For example, R in the form $R_4 = \int P_4(\partial^2 n)^2 dV$[65] contradicts both (A) $(L_M|\partial n| \sim 1)$ and (B) $(|F_2| \sim |R|)$, and $\mathbf{n}$ essentially depends on P_4.

If a finite number of terms in R does not solve the problem, the only possibility which remains is that R in the form of the infinite sum R_∞ satisfies the requirements (A) and (B). It is clear that R_∞ cannot be obtained explicitly. Nevertheless, there are in fact *only two possibilities* to satisfy (A) and (B): either $K_{13} = 0$, or R_∞ behaves in the required fashion. Thus, again the situation seems to be rather paradoxical. Indeed, knowing no explicit expression for R_∞ we have to realize that: (1) the sum $F_2 + R_\infty$ allows only weak deformations; (2) $|R_\infty| \ll |F_2|$, i.e. the series R_∞ converges, though being restricted to any finite order, it might diverge. However, this situation is common rather than any exotic, and the problem of derivative-dependent terms in the anchoring energy will give us an exact example of an infinite sum with all the features required of R_∞.

9.3. *Derivative-dependent terms in the anchoring energy*

Each derivative in the bulk density is accompanied by the small parameter L_M/L, while the anchoring energy contains no scale parameter explicitly. Indeed, ∂n-dependent anchoring terms (46) and (47) were introduced only for the symmetry reason and no magnitude hierarchy in the derivative power occurs in the approach. In Ref. 73 such hierarchy was shown to exist.

On a molecular scale there is an interaction between the nematic molecules and a surface field penetrating inward nematic to some small depth L_S. The idea of the surface field that underlies the introduction of the phenomenological anchoring energy was articulated most explicitly by Sluckin and Poniewierski,[111] Sen and Sullivan,[112] and Osipov.[113]

The surface field directs the nematic molecules along a certain easy direction e, and thus can be considered as a vector $\psi\mathbf{e}$. Its magnitude ψ decreases rapidly along the normal direction so that $\int_0^{Ls} \psi^2 z^k dz \cong \int_0^\infty \psi^2 z^k dz$. Bulk density of the surface-nematic interactions can be written as

$$f_\psi = -\frac{1}{2}W_2(\mathbf{ne})^2\psi^2 + W_4(\mathbf{ne})^4\psi^4 \,. \tag{49}$$

If $\bar{\theta}$ is the angle between the normal k and e, then the quadratic term has the form (with the accuracy fo an n-independent constant)

$$f_{\psi,2} = \frac{1}{2}W_2\psi^2(z)\sin^2[\theta(z) - \bar{\theta}] \,, \tag{50}$$

where $W_2 > 0$. Now the total free energy is given by the sum $F = F_2 + F_{S,2}$, where

$$F_{S,2} = \int dV f_{\psi,2} = \int dS \int_0^\infty dz f_{\psi,2} \,. \tag{51}$$

The elastic constant K_{13} is taken to be zero in this section. Under this condition, the form of Eq. (50) ensures that $f_{\psi,2}$ is bounded from below. The functional $F = F_2 + F_{S,2}$ is minimized by solutions of Euler–Lagrange equations; these equations differ from the Euler–Largange equations of the functional F_2 alone only in a thin subsurface layer of thickness L_s.

Equation (50) represents the surface-nematic interaction as a standard bulk effect. However, we would like to treat the energy density (50) traditionally, i.e. as a purely surface term. Of course, the two representations must be equivalent, i.e. they must lead to the same families of extremals for F, which can in principle differ only in the layer of thickness of order L_S near S. One can pass to the "surface" representation in the following way. Expanding $\sin^2$ in (50) in a power series of z near S given by $z = 0$, $\sin^2[\theta^2(\theta(z)-\bar{\theta}] = \sin^2(\theta_0-\bar{\theta})+z\frac{d\theta_0}{dz}\sin 2(\theta_0-\bar{\theta})+\ldots$, where $\theta_0 = \theta(z=0)$, $\frac{d\theta_0}{dz} = \left(\frac{d\theta}{dz}\right)(z=0)$, we find the surface density of the interaction

$$f_{S,2} = \int_0^\infty dz f_{\psi,2}$$

$$f_{S,2} = \frac{1}{2} W_2 \Bigg\{ \left(\int_0^\infty dz \psi^2 \right) \sin^2(\theta_0 - \bar\theta) + \left(\int_0^\infty dz z \psi^2 \right) \frac{d\theta_0}{dz} \sin\, 2(\theta_0 - \bar\theta)$$

$$+ \frac{1}{2} \left(\int_0^\infty dz z^2 \psi^2 \right) \left[2 \left(\frac{d\theta_0}{dz} \right)^2 \cos\, 2(\theta_0 - \bar\theta) + \frac{d^2\theta_0}{dz^2} \sin\, 2(\theta_0 - \bar\theta) \right] + \dots \Bigg\}.$$

$$(52)$$

Since $\int_0^\infty dz z^k \psi^2 \sim L_S^k \int_0^\infty dz \psi^2 \sim L_S^{k+1}$ and $\frac{d}{dz} \sim 1/L$, Eq. (52) turns out to be the expansion in power series of the small paramter L_S/L. The first term in (52) coincides with the Rapini–Popoular term f_{RP} (45) if the notation $W_{RP} = W_2 \int_0^\infty dz \psi^2$ is introduced. The second term in (52) reproduces f_{DVP} used by Dubois–Violette and Parodi (46); it is L_S/L times smaller than f_{RP}. In the next order of smallness $\sim f_{RP}(L_S/L)^2 \sim f_{DVP}(L_S/L)$, the term $\left(\frac{d\theta_0}{dz} \right)^2 \cos\, 2(\theta_0 - \bar\theta)$ exists, similar to the Mada term (47). The term of the order of $f_{RP}(L_S/L)^3$ and higher are omitted in (52) but of course they can be easily calculated. The term $W_4 (\mathbf{n} \cdot \mathbf{e})^4 \psi^4$ in (49) can be written in the similar form, too.

Formula (52) gives the "surface" representation of the surface-nematic interaction. Of course, Eq. (52) can be thought of as a valid simplification of Eq (48) only if $L_S/L \ll 1$. Then each term of the series (52) has the form const.$\times (L\partial n)_{z=0}^k (L_S/L)^k$, where const.$\sim 1$, $|L\partial n| \sim 1$ by the L-scale definition, and each surface derivative in the anchoring energy is accompanied by a small factor L_S/L, just as each bulk derivative is accompanied by L_M/L. Thus, we obtain a hierarchy of the contributions of derivative-dependent terms in the anchoring energy which now can be classified by order of magnitude.

Since each power of ∂ introduces a small factor in the anchoring energy, the minimization problem for the functional $F = F_2 + F_{S,2}$ can be solved in the form of a power series of this factor by means of perturbation theory. In the lowest-order approximation, the only term contributing to the anchoring energy is the Rapini–Popoular term $F_{RP} = \int dS f_{RP}$. In this approximation, the extremal family of $F = F_2 + F_{RP}$ is the solution of the Euler–Lagrange equations for the functional F_2 which corresponds to the standard weak deformations. The next terms of the series (52) give small corrections of the order of $(L_S/L)^2, (L_S/L)^3$, and so on, and play no practical role as compared with the first approximation.

Let us consider how the surface representation can be treated to minimize the free energy of the nematic sample. The right hand side of formula (52) is the expansion of $f_{S,2}$. Since $f_{\psi,2}$ in Eq. (50) is bounded from below, $f_{S,2} = \int dz f_{\psi,2}$ is bounded too. The results of minimization of the function $f_{S,2}$ itself and its representation as an infinite series must lead to the same weak deformations. Let us, however, truncate this series restricting it to finite power $\bar{k}$ of ∂, and try to minimize such $f_{S,2}^{(\bar{k})}$. Then the same difficulties appear as appeared in the problem of the K_{13} term. Indeed, for any $\bar{k}$ the surface density of the free energy contains the

derivatives of $\bar{k}$ th order. This fact leads to unboundedness of $f_{S,2}^{(\bar{k})}$ from below. This shows that it is impossible to formally restrict the sum R_∞ to any finite number of terms but that it is nevertheless possible that the infinite sum is bounded from below and its minimization results in weak deformations.

What is very important here is that to find n with accuracy $(L_S/L)^2$, it is not necessary to know all the higher terms of the series (52). To demonstrate it further, let us consider an example which is extremely close to the K_{13} problem. To this end we restrict the expansion (52) to $\bar{k} = 1$

$$f_{S,2}^{(1)} = \frac{1}{2} W_{\mathrm{RP}} \sin^2(\theta_0 - \bar{\theta}) + \frac{1}{2} W_{\mathrm{DVP}} \theta_0' \sin\, 2(\theta_0 - \bar{\theta})\,. \tag{53}$$

Formally, (53) results in $|\theta_0'| \longrightarrow \infty$ on S. However, we know that the sum of all the higher-order terms of the series (52) bounds the free energy from below so that θ' is small. Then, since $\theta_0' W_{\mathrm{DVP}} \sim (L_S/L)^2 \ll W_{\mathrm{RP}} \sim L_S/L$, the free energy, corresponding to (53), contains in the first approximation just the first term, and its minimum can be found by solving the Euler–Lagrange equation of the functional F_2. The role of all higher terms is reduced to the restrictions of the functions, upon which $\min[F_2 + \int_{S,2}^{(1)} dS]$ is sought, to the family of solutions of the Euler–Lagrange equation for the functional F_2. The second terms in (53) can be taken into account as a perturbation.

9.4. *Procedure of finding of the director for $K_{13} \neq 0$*

As we saw, the sum F might possess a minimum whereas its first term F_2 has no minimum. Therefore *we must not resort to any features of F_2, and all the assumptions that we can make have to be only about the infinite sum F*. Let us show that if deformations are weak, i.e. $L_M|\partial n| \ll 1$, we can find an approximate equation for them. Indeed, the total free energy expansion has the form $F = F_2 + F_4 + F_6 + \dots$. If F is bounded from below, its extremal family satisfies the Euler–Lagrange equation $D_2 + D_4 + D_6 + \dots = 0$, where $D_{2k} \sim (\partial)^{2k}$ corresponds to F_{2k}. Inasmuch as $L_M\partial \ll 1$, to the order $\sim (L_M\partial)^2$ this equation is merely $D_2 = 0$. This is just the Euler-Lagrange equation of the functional F_2 alone[73] which is similar to the result of the previous section (we remind the reader that Euler–Lagrange equations can be formally written for any functional even if it has no minimum; in our case these equations do not minimize F_2 but appear — one can say accidentally — as certain approximation to the exact minimization procedure). Higher order terms *must* be considered only in the framework of the perturbation theory.

Let a general solution of the equation $D_2 = 0$ be n = n(x, C) where C denotes all the arbitrary parameters. To finally find the director distribution, i.e. to find the values of C, one has to introduce n(x, C) in the functional $F, F\{n(x,C)\} = P(C)$ and then to minimize the function $P(C)$ with respect to C. In the lowest order in small $L_M\partial, P(C) \approx P_2(C) = F_2\{n(x,C)\}$. We see that if deformations

are weak, the information on terms of order higher than 2 enters neither $\mathbf{n}(\mathbf{x}, C)$ nor C,[73] which is just what we required of our theory. *The crucial point is that the consideration given above only assumes the existence of minimum of F and is irrespective of the existence or nonexistnce of minimum of F_2.*

Let us consider the one-dimensional case for the simplest example (Fig. 1): $\mathbf{n} = (\sin\theta, \cos\theta), \theta = \theta(z)$. It corresponds to the sample with two parallel surfaces $S_1(z = z_1)$ and $S_2(z = z_2 > z_1)$. The solution of the Euler–Lagrange equation is $\theta = \theta(z, C_1, C_2)$, its derivative $d\theta/dz = \theta'(z, C_1, C_2)$. Two arbitrary constants C_1 and C_2 can be expressed in terms of the boundary angles θ_1 and θ_2. Introducing functions θ and θ' in the free energy,

$$F_2 = \int_{z_1}^{z_2} f_F dz + \frac{1}{2} K_{13}[\theta'_1 \sin 2(\theta_1 - \bar\theta_1) - \theta'_2 \sin 2(\theta_2 - \bar\theta_2)] + f_A(\theta_2) + f_A(\theta_1) \quad (54)$$

(f_F is given by Eq. (2) and f_A is the anchoring energy), we minimize the obtained function of θ_1 and θ_2 with respect to these angles. Employing notations $A_1 = A(z = z_1)$ and $A_2 = A(z = z_2)$ for any function $A(z)$, we find two equations with respect to the two constants θ_1 and θ_2[73]

$$\left(\frac{\partial f_F}{\partial \theta'}\right)_1 - \left(\frac{\partial f_A}{\partial \theta}\right)_1 - K_{13}\left[\theta'_1 \cos 2\theta_1 + \frac{1}{2}\sin 2\theta_1 \frac{d\theta'_1}{d\theta_1} - \frac{1}{2}\sin 2\theta_2 \frac{d\theta'_2}{d\theta_1}\right] = 0,$$

$$\left(\frac{\partial f_F}{\partial \theta'}\right)_2 + \left(\frac{\partial f_A}{\partial \theta}\right)_2 - K_{13}\left[\theta'_2 \cos 2\theta_2 + \frac{1}{2}\sin 2\theta_2 \frac{d\theta'_2}{d\theta_2} - \frac{1}{2}\sin 2\theta_1 \frac{d\theta'_1}{d\theta_2}\right] = 0.$$
$$\quad (55)$$

The last term in each equation comes from the fact that $d\theta'_1/d\theta_2$ and $d\theta'_2/d\theta_1$ do not vanish (while $d\theta_1/d\theta_2 = d\theta_2/d\theta_1 \equiv 0$). These last terms, which have been always missing in previous versions of boundary conditions,[104–107,114–118] couple variations of the angles on different boundaries due to the presence of the derivative in the surface part of the free energy. In particular, it is easy to see that if these terms are missing, the K_{13} contribution plays the role of an intrinsic deformation source even for $\theta_1 = \theta_2$, and Eqs. (55) result in unphysical distortions under no external cause. A very large value of the constant K_{13} obtained in experiment[115] has to be attributed to such the incorrect version of Eqs. (55) employed in this paper.

9.5. *Geometrical structure of the surfacelike terms*

Since the basic question I from Sec. 8 is answered positively, the question II becomes meaningful. The crucial difference between the K_{13} and K_{24} terms is their different geometrical structure.[71,73] For arbitrary surface S of a nematic sample, the K_{24} term (5) contains only derivatives $\partial_\parallel n$ in the directions tangential to S and does not contain derivatives $\partial_\perp n$ along the normal direction; the K_{13} term f_{13} (4) always contains the director derivatives $\partial_\perp n$ normal to S. It is this normal derivative that becomes infinite, resulting in an unboundedness of the functional (1) from below.

The geometrical structure of the surfacelike terms suggests that it is convenient to rearrange their contribution in a way which is even more natural than separating into the K_{13} and K_{24} terms. Namely, it is convenient to separate the normal and tangential derivatives in the total contribution, $f_{13} + f_{24} = f_{S,\parallel} + f_{S,\perp}$.[73] Then the most essential part of the K_{13} term is[73]

$$f_{S,\perp} = \frac{K_{13}}{\sqrt{g_{\alpha\beta}k_\alpha k_\beta}}(\mathbf{kn})(\mathbf{k}\nabla)(\mathbf{kn}), \tag{56}$$

where $g_{\alpha\beta}$ is the metric tensor of the coordinate system employed, $\mathbf{k}$ is a unit external normal to S, and a summation is implied over repeating subscripts. If the coordinate system is chosen so that the surface S is normal to the x_3-lines, then

$$f_{S,\perp} = \frac{k_{13}n_3\partial_3 n_3}{\sqrt{g_{33}}}. \tag{57}$$

9.6. *Vanishing of contribution of the K_{13} term to the balance of mechanical torques*

Formula (56) explicitly depends on the surface normal $\mathbf{k}$ and thus is invariant with respect to rotations of the sample as a whole (or the coordinate system). For some general problems this is very important. For example, let us consider mechanical torque that is applied to the surface of the nematic sample due to presence of the K_{13} term. To find the α-component τ_α of the torque one has[15,63]: (1) to rotate the director, the surface and the coordinate system through the same infinitesimal angle ω_α about the α-axis (in Cartesian coordinates); (2) to write the transformed free energy F'; (3) to expand the difference $F'\{\mathbf{n}'(\mathbf{x}'), \mathbf{k}'\} - F\{\mathbf{n}(\mathbf{x}), \mathbf{k}\}$ in power series of ω_α. The first order term in ω_α is $\tau_\alpha\omega_\alpha$ which is the mechanical work expended in order to rotate the sample.

In the one-dimensional case the surfaces are planes and the metric tensor is trivial, $g_{\alpha\beta} = \delta_{\alpha\beta}$, while components of the vecotrs $\mathbf{x}, \mathbf{k}$ and ∇ before the rotation are given by

$$\mathbf{x} = (x, y, z) = (x_1, x_2, x_3),$$

$$\mathbf{k} = (0, 0, 1), \tag{58}$$

$$\nabla = (0, 0, \partial_3).$$

The K_{13} contribution to the free energy is $F_{13} = \int dS f_{S,\perp}(k_\alpha, n_\alpha)$ where $f_{S,\perp} = K_{13}(\mathbf{kn})(\mathbf{k}\nabla)(\mathbf{kn})$. To obtain $F'_{13} = \int dS' f_{S,\perp}(\mathbf{n}'(\mathbf{x}'), \mathbf{k}')$ we rotate the sample shown in Fig. (1), i.e. the vector k_α and director n_α, and the coordinates x_α. The surface area S is a scalar, $S' = S$. Introducing vector $(\omega_1, \omega_2, \omega_3)$ of the rotation angles and the unit antisymmetric tensor $\varepsilon_{\alpha\beta\gamma}$ we can write the transformed vector

components as

$$x'_\alpha = x_\alpha + \varepsilon_{\alpha\beta\gamma}\omega_\beta x_\gamma\,, \tag{59}$$

$$n'_\alpha(\mathbf{x}) = n_\alpha(\mathbf{x}) + \varepsilon_{\alpha\beta\gamma}\omega_\beta n_\gamma\,, \tag{60}$$

$$k'_\alpha = k_\alpha + \varepsilon_{\alpha\beta\gamma}\omega_\beta k_\gamma\,. \tag{61}$$

For any scalar function $A(\mathbf{n}(\mathbf{x}),\mathbf{k})$ the total variation δA under transformation (59)–(61) is defined as

$$\delta A = A(\mathbf{n'}(\mathbf{x'}),\,\mathbf{k'}) - A(\mathbf{n}(\mathbf{x}),\,\mathbf{k})\,.$$

It is also convenient to introduce the quantity $\bar{\delta}A$ (the so-called form variation[63]) in which $\mathbf{n'}(\mathbf{x'})$ is replaced by $\mathbf{n'}(\mathbf{x})$, i.e.

$$\bar{\delta}A = A(\mathbf{n'}(\mathbf{x}),\,\mathbf{k'}) - A(\mathbf{n}(\mathbf{x}),\,\mathbf{k})\,.$$

To the first order in the small parameters ω_α of the transformations these variations are evidently related as

$$\delta A = \bar{\delta}A + \frac{\partial A}{\partial x_\alpha}\delta x_\alpha\,. \tag{62}$$

The function $f_{S,\perp}$ depends only on the combinations $(\mathbf{kn})$ and $(\mathbf{k}\nabla)(\mathbf{kn})$ and does not depend on $\mathbf{x}$ explicitly. Therefore, the difference $\delta f_{S,\perp}$ in the K_{13} density (56) due to the transformation (59)–(61) can be written as

$$\begin{aligned}
\delta f_{S,\perp} &= f_{S,\perp}(\mathbf{k'}(\mathbf{x'}),\,\mathbf{n'}(\mathbf{x'})) - f_{S,\perp}(\mathbf{k}(\mathbf{x}),\,\mathbf{n}(\mathbf{x})) \\
&= \frac{\partial f_{S,\perp}}{\partial(\mathbf{kn})}\delta(\mathbf{kn}) + \frac{\partial f_{S,\perp}}{\partial[(\mathbf{k}\nabla)(\mathbf{kn})]}\delta[(\mathbf{k}\nabla)(\mathbf{kn})] \\
&= \frac{\partial f_{S,\perp}}{\partial(\mathbf{kn})}\bar{\delta}(\mathbf{kn}) + \frac{\partial f_{S,\perp}}{\partial(\mathbf{k}\nabla)(\mathbf{kn})}\bar{\delta}[(\mathbf{k}\nabla)(\mathbf{kn})] + \frac{df_{S,\perp}}{dx_\alpha}\bar{\delta}x_\alpha \\
&\equiv \bar{\delta}f_{S,\perp} + \frac{df_{S,\perp}}{dx_\alpha}\bar{\delta}x_\alpha\,, \tag{63}
\end{aligned}$$

where we employed Eq. (62). The form variations entering Eq. (63) are

$$\bar{\delta}(\mathbf{kn}) = (\mathbf{k'n'}(\mathbf{x})) - (\mathbf{kn}(\mathbf{x}))\,, \tag{64a}$$

$$\begin{aligned}
\bar{\delta}[(\mathbf{k}\nabla)(\mathbf{kn})] &= (\mathbf{k'}\nabla')(\mathbf{k'n'}(\mathbf{x})) - (\mathbf{k}\nabla)(\mathbf{kn}(\mathbf{x})) \\
&= (\mathbf{k'}\nabla' - \mathbf{k}\nabla)(\mathbf{kn}(\mathbf{x})) + (\mathbf{k'}\nabla')\bar{\delta}(\mathbf{kn})\,.
\end{aligned} \tag{64b}$$

Equation (61), along with the fact that, by virtue of scalars,

$$(\mathbf{k'}\nabla') - (\mathbf{k}\nabla) = (\mathbf{k'n'}(\mathbf{x'})) - (\mathbf{kn}(\mathbf{x})) = 0\,,$$

allows one to reduce Eqs. (64) to the from

$$\bar{\delta}(\mathbf{kn}) = -\left(\mathbf{k}'\frac{\partial \mathbf{n}'(\mathbf{x})}{\partial x_\alpha}\right)(x'_\alpha - x_\alpha), \tag{65a}$$

$$\bar{\delta}[(\mathbf{k}\nabla)(\mathbf{kn})] = -(\mathbf{k}\nabla)\left[\left(\mathbf{k}'\frac{\partial \mathbf{n}'(\mathbf{x})}{\partial x_\alpha}\right)(x'_\alpha - x_\alpha)\right]. \tag{65b}$$

Then, substituting Eqs. (65) into the definition of $\bar{\delta}f_{S,\perp}$ (Eq. (62)) and making use of Eqs. (58) and (59) one obtains

$$\bar{\delta}f_{S,\perp} = K_{13}\omega_2 x_1 \partial_3(n_3\partial_3 n_3). \tag{66}$$

At the same time, a straightfroward calculation of the second term in the last line of Eq. (63) gives exactly expression (66) but with the opposite sign, i.e.

$$\frac{\partial f_{S,\perp}}{\partial x_\alpha}\delta x_\alpha = -K_{13}\omega_2 x_1 \partial_3(n_3\partial_3 n_3).$$

Thus, the contribution $\tau_{\alpha,13}$ of the K_{13} term to the balance of mechanical torques vanishes identically, irrespective of the director distribution in the bulk:

$$\delta f_{S,\perp} = \delta F_{13} \equiv 0. \tag{67}$$

Although formula (57) corresponds to the chosen coordinate system, its use would have led to a nonvaishing torque, in contrast to the correct result (67) based on Eq. (56). The point is that rotation (61) of the normal to the surface does not affect the free energy (57) since the normal k does not enter Eq. (57). Therefore, transformations (59)–(61) of the free energy in form (57) correspond to the rotation of the director alone while the surface is fixed. In this case, the nonvanishing torque is not a surprise. We see that general transformations must be performed only in the covariant formula (56).

It is relevant to mention here that the derivation of the expression for elastic torque cannot be simplified by including into consideration some external field. For example, suppose that magnetic field $\mathbf{H}_\Omega$ is applied to the sample whose direction makes the angle Ω with the z-axis. Then, the equilibrium director depends on Ω, i.e. $\mathbf{n} = \mathbf{n}(\mathbf{x}, \Omega)$. If the sample is rotated through the angle ω according to Eqs. (59)–(61), the transformed system can be descibed as $\mathbf{n}_1 = \mathbf{n}' = \mathbf{n}_\omega(\mathbf{x}, \Omega), \mathbf{H}_1 = \mathbf{H}_\Omega$ (case 2) (we emphasize that $\mathbf{n}_1 = \mathbf{n}_\omega(\mathbf{x}, \Omega)$ is a so-called virtual state, i.e. is an equilibrium distribution neither for $\mathbf{H}_1 = \mathbf{H}_\Omega$ nor for $\mathbf{H}_1 = \mathbf{H}_{\Omega+\omega}$). Since ω enters the director, taking the derivative of δF with respect to ω we obtain the standard expression for elastic torque and its balance with the magnetic torque.[15] Physically, the state equivalent to that of case 1 obtains also by the rotation of the magnetic field through the angle $(-\omega)$ *while the director is fixed*: $\mathbf{n}_2 = \mathbf{n}(\mathbf{x}, \Omega), \mathbf{H}_2 = \mathbf{H}_{\Omega+\omega}$ (case 1) (again, $\mathbf{n}_2$ has nothing to do with the equilibrium distribution corresponding

to H_2). Then, however, in contrast to case 1 the angle ω does not enter n_2, and hence the elastic contribution to the torque cannot be derived in case 2. Rather, the procedure employed in case 2 enables one to derive expression for the magnetic torque (since ω enters H_2) and its balance with the torque applied to the magnet.

Recently it has been argued[118] that the procedure of field rotation results in a nonzero K_{13} contribution to the balance of torques. Nonzero K_{13} contribution was obtained in Ref. 118 because *the ω-independent* n_2 *was incorrectly replaced by the ω-dependent* $n_F = n(x, \Omega+\omega)$. This n_F is the equilibrium director corresponding to $H_2 = H_{\Omega+\omega}$ rather than to $H_1 = H_\Omega$ as it must be (the state $n_F = n(x, \Omega+\omega)$, $H_2 = H_{\Omega+\omega}$ is *equilibrium rather than virtual*). This state "F" differs from those of case 2, and, thus, is not equivalent to case 1. Therefore, the procedure employed in Ref. 118 differs from those required by the general principle of mechanics.

9.7. Anomalous Fréedericksz effect and spontaneous parity violation induced by the K_{13} term

As was shown in Sec. 9.4, the equilibrium director configuration is given to order $(\delta n)^2$ by the Euler–Lagrange equations for the functional F_2 (1). Moreover, no information on R_∞ is required; hence, no more constants need to be introduced into the theory. The surfacelike elastic constants are shown to be unambiguous from a microscopic point of view.[66] On the other hand, since all ∂n-dependent terms in the anchoring energy are much smaller than the Rapini–Popoular and K_{13} terms, we can neglect extrinsic ∂n-dependent contributions and thereby assign well-defined values to the surfacelike elastic constants. We thus seek an experimental situation in which K_{13} would play a prominent role. One such effect is predicted in the standard Fréedericksz geometry.[119,120] In these papers, a flat nematic film is considered sandwiched between two surfaces $z = \pm h/2$ with homeotropic anchoring of equal strength W. The linearized Euler–Lagrange equation of the problem has a solution

$$\theta(z) = A \sin qz + N \cos qz, \qquad q = \sqrt{\chi_\alpha H^2/K_{33}}, \qquad (68)$$

where H is the magnetic field strength, and $\chi_\alpha > 0$. In the standard treatment of the Fréedericksz transition, it is assumed that because of the symmetry of the problem, only the even solution $\theta_N(z) = N \cos qz$ should be retained. However, for sufficiently large K_{13}, a parity-breaking mode $\theta_A(z) = A \sin qz$ can be excited which is odd with respect to $z = 0$ (Fig. 12).

If $K_{33} > 2K_{13}$ only the N mode can be excited. The only difference with the standard Fréedericksz transition is that the nonzero K_{13} shifts the threshold since K_{33} is replaced by $K_{33,\text{eff}} = K_{33} - 2K_{13}$.

What happens if $K_{33,\text{eff}}$ is negative, i.e. $K_{33} < 2K_{13}$? The answer depends on the thickness of the layer. If the layer is thin enough, $h < h_c = 2(2K_{13} - K_{33})/W$, then the director behaves as if it has a negative bend constant so that energy has to be expended in order to produce an undistorted (U) state. The A mode spontaneously occurs for zero H. The amplitude A decreases with an increase of H and vanishes
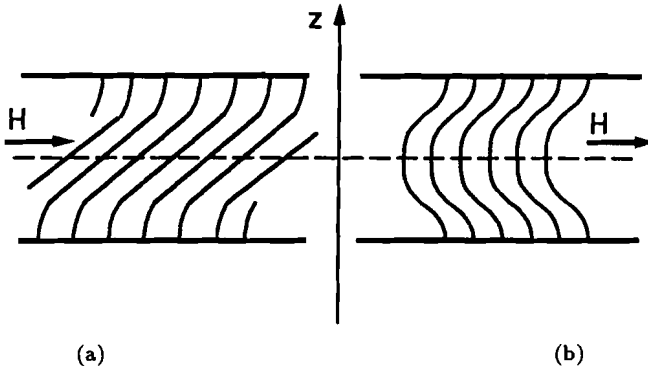
Fig. 12. Normal (a) and parity-breaking (b) distortion modes of a thin nematic film with normal anchoring at both interfaces.

(undistorted state (U)). Then, for some H, the N mode appears, its amplitude N first increases and, upon reaching a maximum, decreases down to zero. After the U regime the A mode appears again and so on.

If $K_{33} < 2K_{13}$, but $h > h_c$, then the A mode is not excited, and instead of the sequence A–U–N–U–A–... a sequence of the states is U–N–U–N–.... The case of the initial planar alignment is similar but the critical conditions for the A mode and the anomalous behavior are now $2|K_{13}| > K_{33}, K_{13} < 0$.[119,120]

Thus, small K_{13} just shifts the critical field of the standard Fréedericksz transition. Large K_{13} can cause spontaneous parity violation of n in sufficiently thin films and anomalous Fréedericksz effect in which the applied field alternatively enhances and inhibits distortions. The fact that the anomalous effect is not observed at worst implies that $|K_{13}| < K_{33}/2$ for the studied materials. Note that recent experiments performed for the stripe domain phase in nematic LLC films suggested that for 5CB $K_{13} \approx -0.2\, K_{11}$.[121] We consider below the influence of the K_{13} term on the stripe domain phase.

9.8. *Stripe domain spectrum and the K_{13} elasticity*

The results of previous sections enable one to include the K_{13} term in the theory of stripe domain phase of Sec. 5.4. General scheme and formulae remain the same as for $K_{13} = 0$. In presence of a nonvaishing K_{13}, Eqs. (11) and (12), which determine the boundary angles in the homogeneous one-dimensional state, are replaced by Eqs. (55) which read

$$2(\theta_2 - \theta_1) + h(W_2/K)\sin 2\theta_2 = p_\perp[(\theta_2 - \theta_1)\cos 2\theta_2 + \frac{1}{2}(\sin 2\theta_2 - \sin 2\theta_1)], \tag{69}$$

$$2(\theta_2 - \theta_1) + h(W_1/K)\sin 2\theta_1 = p_\perp[(\theta_2 - \theta_1)\cos 2\theta_1 + \frac{1}{2}(\sin 2\theta_2 - \sin 2\theta_1)], \tag{70}$$

where $p_\perp = 2K_{13}/K$. The critical thickness (10) of the transition between the distorted and undistorted homogeneous states becomes[122]

$$h_a = K(1/W_2 - 1/W_1)(1 - p_\perp), \tag{71}$$

The factor $|1-p|$ is now replaced by $p_\parallel = |1-(2K_{24}-K_{13})/K|; p_\perp$ and $p_\parallel$ correspond to the total contributions of the director derivatives along normal and tangential directions to the surfaces, respectively, i.e. to $f_{S\perp}$ and $f_{S,\parallel}$ introduced in Ref. 73 (Sec. 8.5).

The transition homogeneous state-stripe domain state is of the second order and for $\chi \ll 1$ can be described by the functional[45]

$$F\{G(u)\} = \frac{K_{11}}{4\pi} \int_0^{2\pi} du \left[\chi^4 \lambda D G'^2 + \chi^6 \left(P G''^2 + Q G^2 G'^2 \right) \right], \tag{72}$$

whose coefficients λ, D, P, Q are unambiguously determined by the solution θ_1, θ_2 of Eqs. (69) and (70); $u = 2\pi y$. The perturbations are related to the function $G(u)$ and its derivative G' as $\varphi = \chi G + O(\chi^3)$, $\psi = -\chi^2(\alpha - \beta z)G' + O(\chi^4)$, where α and β are u-independent constants. Minimization of functional (72) results in a periodic solution $G(u)$ with the wave number

$$\chi = 2\pi h/L = \sqrt{-0.4\,D\lambda\,/\,3P}, \tag{73}$$

where the coefficient 0.4 results from nonlinear interaction of the harmonics. As it is seen from Eq. (73) the stripe domains with $\chi \ll 1$ do not exist for $Q \leq 0$ since in this case $\min F\{G(u)\}$ corresponds to $\chi \to \infty$. The inequality $Q > 0$ takes place for $h < h_Q$, where h_Q is defined by $Q(h_Q) = 0$ which implies that the long-wavelength domain phase exists only for $h < h_Q$. Thus, Eq. (73) together with the value of h_Q completely determines the long-wavelength spectrum.

The function $\chi(h)$ possesses the following features. Its zeros h_d and h_u are the roots of $D(h)$. Hence $D < 0$ and $D > 0$ correspond to the domain and homogeneous states, respectively. The inequality $D < 0$ holds for $h_d < h < h_u$. Of course, this picture is meaningful only below h_Q: the upper boundary of the domain phase is $h_c = \min(h_u, h_Q)$. If $h_c = h_u$, then at the right end of the spectrum χ vanishes as $(h_u - h)^{1/2}$, which is illustrated by curves 1–3 in Fig. 13; if $h_c = h_Q$, then $\chi(h)$ jumps up abruptly (curve 4 in Fig. 13). An exact analytical formula can be found for the lower boundary h_d of the spectrum, i.e.

$$h_d = \max \left[h_a(1 - \frac{p_\parallel^2}{1 - p_\perp}), 0 \right], \tag{74}$$

while the upper boundary h_c can be found only numerically from transcendental Eqs. (69) and (70), and $D = Q = 0$. The single maximum of χ at h_m is always somewhat rightward h_a. An important scaling parameter of the spectrum is the
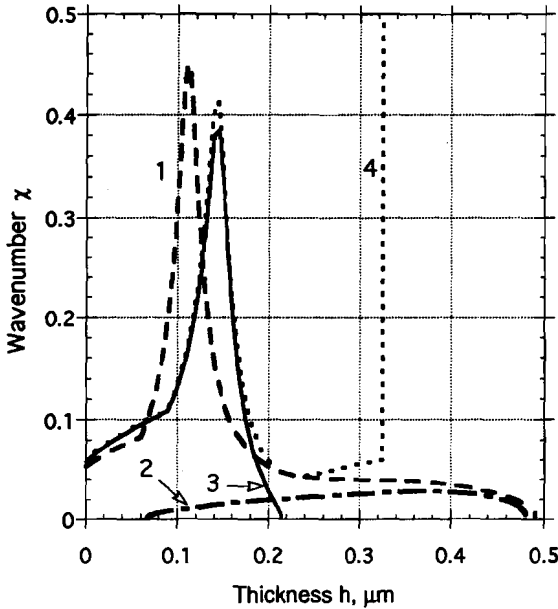
Fig. 13. Wavenumber χ of the stripe domain phase as a function of film thickness calculated using Eq. (73) and the following parameters: (1) $K_{13} = -0.205K_{11}$, $L_1 = 0.76\,\mu$m, $L_2 = 0.86\,\mu$m, $h_a = 0.06\,\mu$m, $p_{\|} = 1.0$; (2) $K_{13} = 0$, $L_1 = 6.65\,\mu$m, $L_2 = 7\,\mu$m, $h_a = 0.35\,\mu$m, $p_{\|} = 0.9$; (3) $K_{13} = 0$, $L_1 = 0.61\,\mu$m, $L_2 = 0.76\,\mu$m, $h_a = 0.09\,\mu$m, $p_{\|} = 1.187$; (4) $K_{13} = 0$, $L_1 = 0.61\,\mu$m, $L_2 = 0.7\,\mu$m, $h_a = 0.09\,\mu$m, $p_{\|} = 1.2$; $t = 0.63$ for all the curves.

ratio $\eta = h_c/h_m$. If $L_1 - L_2 \sim L_1 \sim L_2$ this paramter is close to 1 (curve 2); the larger η can occur only if $h_a \ll L_1, L_2$, which is the case for $L_2 - L_1 \ll L_1, L_2$ (curve 1, Fig. 13).

The general picture is that increase of $p_{\|}$ causes both an increase of h_u and substantial decrease of h_s (compare curves 4 and 3). Depending on the other parameters of the problem, these two effects may shift the upper end h_c of the spectrum towards larger or smaller h. Negative K_{13} favors growth of both h_c and η. This is illustrated in Fig. 13.

High sensitivity of the stripe domain spectrum to small variations of K_{13} and K_{24} (Fig. 13) allows one to anticipate that both K_{13} and K_{24} can be found by comparison of theoretical and experimental curves $\chi(h)$. Such an experiment was performed recently.[121] It turned out that the agreement between the experimental and theoretical curves $\chi(h)$ can be provided only when $K_{13} \neq 0$. For 5CB it was found that $K_{13} \approx -0.2K_{11}$ and $K_{24} \approx -0.1K_{11}$ or $K_{24} \approx 0.9K_{11}$ (the two values of K_{24} emerge because only the absolute value $p_{\|}$ enters the theory). Curve 1 in Fig. 13 corresponds to the best fit of the experimental data (for more details, see Ref. 121).

The stripe domains are not the only example of periodic patterns in the LLC films. Figure 14 shows two other typical textures: cellular patterns formed by
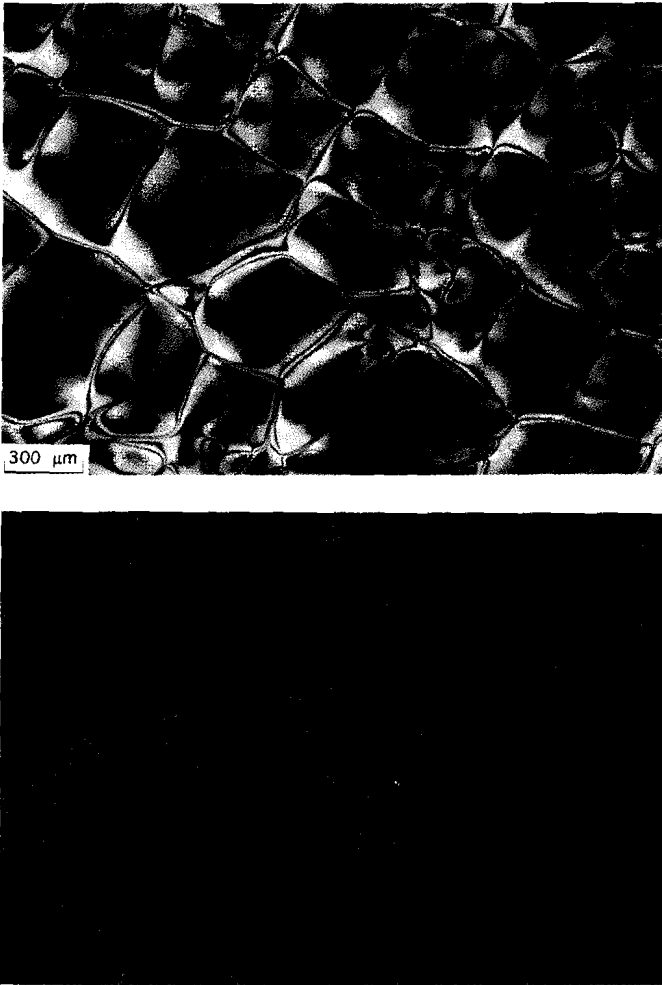
Fig. 14. Cellular patterns with strings that do not erminate at the singular points, $h \approx 4 \, \mu$ m (a) and lattice of point defects, $h \approx 0.3 \, \mu$ m (b) (5CB/glycerin).

strings and a lattice of point defects. Note that these strings do not terminate at point defects (as strings shown in Fig. 6). An intriguing beauty of patterns in the LLC films is a real challenge for the theory of liquid crystals.

10. Conclusion

The present situation with K_{13} and K_{24} is similar to that of the K_{22} elastic constant about thirty years ago when its value was not known.[123] Over these years joint efforts of the theoretical macroscopic approach and experiment have made the twist elasticity a well-defined physical idea and K_{22} a reliably measured quantity. We believe that the same approach will allow us to comprehend the nature of the

divergence or "surfacelike" elasticity of liquid crystals. Each subject, however, requires of the researcher first to find the physical situations where the phenomena under investigation would be most pronounced and could have led to qualitatively new effects. The LLCs represent such physical situations for the surfacelike elasticity of the nematic phase: the majority of the considered structures are caused by the particular mechanisms of spontaneous symmetry violation associated with the divergence terms.

The LLC geometry is useful to study the surface/bulk balance also in layered liquid crystals such as SmA. We did not consider the SmC LLC films in this review, but preliminary results[124] indicate that non-chiral SmC films placed on a glycerin surface reveal many striking patterns similar to that in the nematic films (high-strength defects, strings and periodic domains). The patterns in SmC films might be also connected with the divergence elasticity and hybrid character of alignment. The last assumption is supported by the observation of high-strength defects in SmC and SmF films with free surface placed on glass substrates.[125]

There are a number of reports on striped patterns in thin SmC films either freely suspended in air[126] or deposited on a rigid substrate with unidirectional azimuthal anchoring.[127] Theoretical models[5,128,129] explained the stripe domains of SmC freely suspended films as a result of chiral nature of the molecules. However, there are recent observations of the stripe domain phase in hexatic liquid crystal films[7] and in Langmuir monolayers[130,131] composed of *nonchiral* molecules. These stripe domains can be explained as a result of the up-down asymmetry of the films.[132,133,130,7] Therefore, the symmetry breaking mechanism in SmC films and Langmuir monolayers is quite similar to the divergence (K_{24}) mechanism described for the stripe phase in non chiral nematic films jplaced between two different media (see Refs. 35, 45, 46 and 121 and Sec. 5.4 of the present review). In fact, by representing the director n through its projection onto the film plane c, it is easy to see that the K_{13} and K_{24} terms in the three-dimensional Frank–Oseen elastic functional produce terms such as $\nabla \cdot c$[134] responsible for the splay-stripes in the two-dimensional elastic theory.[133]

From the experimental point of view, the LLCs enable one to apply optical methods including microscopy to study essentially submicrometer phenomena. The parameters of the system (temperature, film thickness, boundary conditions) can be controlled. From the theoretical point of view, the LLCs give the unqiue opportunity to study the general problem of divergence terms in free energy functionals. Heuristic importance of such an investigation is not restricted only to liquid crystals. It might, in principle, point to the situations in other areas of physics where surfacelike terms are meaningful (e.g., ferromagnets).

The physical content of the LLCs in not, however, exhausted by the problem of the divergence elasticity. Since in many cases the shape of the liquid crystalline film is not flat, the pattern formation can be strongly affected by the geometrical anchoring.[42] On the other hand, the method of the LLCs preparation in the Langmuir trough can be used to study the mechanisms of the physcial anchoring,

since the parameters of the system (e.g. presence of surfactant, concentration of ions, film thickness, density) can be easily modified and controlled. Other physical mechanisms that govern behavior of the LLCs are connected with flexoelectricity and surface polarization that might occur at the interface because of the ferroelectric ordering and presence of ions.

Acknowledgments

References

1. P. G. de Gennes, *Rev. Mod. Phys.* **57**, 827 (1985).
2. L. Leger and J. F. Joanny, *Rep. Prog. Phys.* **56**, 431 (1992).
3. C. Y. Young, R. Pindak, N. A. Clark, and R. Meyer, *Phys. Rev. Lett.* **40**, 773 (1978).
4. J. D. Brock, A. Aharony, R. Birgenau, K. Evans-Lutterodt, J. D. Litster, P. M. Horn, G. B. Stephenson and A. R. Tajbakhsh, *Phys. Rev. Lett.* **57** 98 (1986).
5. G. A. Hinshaw, R. G. Petschek and R. A. Pelcovits, *Phys. Rev. Lett.* **60**, 1864 (1988); G. A. Hinshaw and R. G. Petschek, Phys. Rev. **A39**, 5914 (1989).
6. P. S. Pershan, *Structure of Liquid Crystal Phases* (World Scientific, Singapore, (1988).
7. J. Maclennan and M. Seul, *Phys. Rev. Lett.* **69**, 2082 (1992); **69**, 3267 (E) (1992); J. Maclennan, U. Sohling, N. A. Clark and M. Seul, *Phys. Rev.* **E49**, 3207 (1994).
8. R. Geer, T. Stabe, C. C. Huang, R. Pindak, J. W. Goodby, M. Cheng, J. T. Ho and S. W. Hui, *Nature* **355**, 152 (1992).
9. I. Kraus, P. Pieranski, E. Demikhov, H. Stegemeyer and J. Goodby, *Phys. Rev.* **E48** 1916 (1993).
10. D. Meyerhofer, A. Sussman and B. Williams, *J. Appl. Phys.* **43**, 3685 (1972).
11. S. Faetti and L. Fronsoni, *Solid State Commun.* **25**, 1087 (1978).
12. H. Möhwald, *Rep. Prog. Phys.* **56** 653 (1993).
13. D. Andelman, F. Brochard, Ch. M. Knobler and F. Rondelez, *Modern Amphiphilic Physics,* ed. A. Ben-Shaul, D. Roux and W. M. Galbart, Ch. 12 (1993).
14. I. R. Peterson, *J. Mol. Electron.* **2**, 95 (1986).
15. P. G. de Gennes and J. Prost, *The Physics of Liquid Crystals* (Clarendon Press, Oxford, 1993).
16. M. Kléman, *Points, Lines and Walls in Liquid Crystals, Magnetic Systems and Various Ordered Media* (Wiley, New York, 1983).
17. J. W. Doane, in *Liquid Crystals: Applications and Uses,* vol. 1, ed. B. Bahadur (World Scientific, N.J., 1990), Chap. 14; *MRS Bulletin* **16** 22 (1991).
18. F. M. Aliev, *Lzvestiya Akademii Nauk SSR. Ser. Fiz.,* **53** 1904 (1989). [*Bull. Acad. Sci. USSR, Phys. Ser.* **53** 45 (1989)]; *Mol. Cryst. Liq. Cryst.* (1994, in press).
19. A. Golemme, S. Zumer, D. W. Allender and J. W. Doane, *Phys. Rev. Lett.* **61**, 2937 (1988).
20. M. V. Kurik and O. D. Lavrentovich, *Usp. Fiz. Nauk* **154**, 381 (1988) [*Sov. Phys. Uspekhi* **31**, 196 (1988)].
21. D. W. Allender, G. P. Crawford and J. W. Doane, *Phys. Rev. Lett.* **67**, 1442 (1991).
22. G. P. Crowford, D. W. Allender and J. W. Doane, *Phys. Rev.* **A45**, 8693 (1992).

23. R. Ondris-Crawford, G. P. Crawford, S. Zumer and J. W. Doane, *Phys. Rev. Lett.* **70**, 194 (1993).
24. R. D. Polak, G. P. Crawford, B. C. Kostival, J. W. Doane and S. Zumer, *Phys. Rev.* **E49**, R978 (1994).
25. X. -L. Wu, W. I. Goldburg, M. X. Liu and J. A. Xue, *Phys. Rev. Lett.* **69**, 470 (1992).
26. G. Iannachione and D. Finotello, *Phys. Rev. Lett.* **69**, 2094 (1992).
27. G. Crawford, R. Ondris-Crawford, S. Zumer and J. W. Doane, *Phys. Rev. Lett.* **70**, 1838 (1993).
28. B. Jérôme and M. Boix, *Phys. Rev.* 15A **45**, 5746 (1992).
29. E. G. Bortchagovsky and L. N. Tarakhan, *Phys. Rev.* **B47**, 2431 (1993).
30. M. J. Press and A. S. Arrott, *Phys. Rev. Lett.* **33**, 403 (1974); *J. Phys. (Fr.)* **36**, C1-177 (1975).
31. J. Proust, E. Perez and L. Terminassian-Saraga, *Coll. Pol. Sci.* **255**, 1003 (1978); **256**, 784 (1978).
32. O. D. Lavrentovich and Yu. A. Nastishin, *Ukrainian Fiz. Zhurn.* **32**, 710 (1978).
33. O. D. Lavrentovich and S. S. Rozhkov, *Pis'ma Zh. Eksp. Teor. Fiz.* **47**, 210 (1988).
34. O. D. Lavrentovich and V. M. Pergamenschik, *Pis'ma Zhurn. Tekhn. Fiz.* **15**, 73 (1989) [*Sov. Tech. Phys. Lett.* **15**, 194 (1989)]; [JEPT Lett. **47**, 254 (1988)].
35. O. Lavrentovich and V. Pergamenshchik, *Mol. Cryst. Liq. Cryst.* **179**, 125 (1990).
36. O. D. Lavrentovich and Yu. A. Nastishin, *Europhys. Lett.* **12**, 135 (1990).
37. O. D. Lavrentovich, *Mol. Cryst. Liq. Cryst.* **191**, 77 (1990).
38. A. Sparavigna, L. Komitov, B. Stebler and A. Strigazzi, *Mol. Cryst. Liq. Cryst.* **207**, 265 (1991).
39. O. D. Lavrentovich, *Physica Scripta* **T39**, 394 (1991).
40. A. Sparavigna and A. Strigazzi, *Mol. Cryst. Liq. Cryst.* **221**, 109 (1992).
41. A. Sparavigna, L. Komitov and A. Strigazzi, *Mol. Cryst. Liq. Cryst.* **212**, 289 (1992).
42. O. D. Lavrentovich, *Phys. Rev. A15* **46**, R722 (1992).
43. A. Sparavigna, L. Komitov, O. D. Lavrentovich and A. Strigazzi, *J. Phys. (Paris)* II **2**, 1881 (1992); A. Sparavigna, O. D. Lavrentovich and A. Strigazzi, *Phys. Rev.* **E** submitted (1994).
44. O. D. Lavrentovich, *Liquid Crystals Today* **2**, 4 (1992).
45. V. M. Pergamenshchik, *Phys. Rev.* **E47**, 1881 (1993).
46. A. Sparavigna, O. D. Lavrentovich and A. Strigazzi, *Phys. Rev.* **E49**, 1344 (1994).
47. P. Guyot-Sionnest, H. Hsiung, and Y. R. Shen, *Phys. Rev. Lett.* **57**, 2963 (1986).
48. R. B. Meyer, *Mol. Cryst. Liq. Cryst.* **16**, 355 (1972).
49. H. Yokoyama, S. Kobayashi and H. Kamei, *Mol. Cryst. Liq. Cryst.* **99**, 39 (1983).
50. N. V. Madhusudana and K. R. Sumathy, *Mol. Cryst. Liq. Cryst.* **129**, 137 (1985).
51. J. B. Fournier, I. Dozov and G. Durand, *Phys. Rev.* **A41**, 2252 (1990).
52. P. G. de Gennes, *Solid State Commun.* **8**, 213 (1970).
53. O. D. Lavrentovich and L. N. Tarakhan, *Zhurn. Tekh. Fiz.* **56**, 2071 (1986). [*Sov. Phys. Tech. Phys.* **31**, 1244 (1986)]; *Poverkhnost* **1**, 39 (1990).
54. S. Faetti, *Mol. Cryst. Liq. Cryst.* **129**, 137 (1985).
55. L. M. Blinov, E. I. Kats and A. A. Sonin, *Usp. Fiz. Nauk* **152**, 449 (1987) [*Sov. Phys. Uspekhi* **30**, 604 (1987)]; B. Jérôme, *Rep. Prog. Phys.* **54**, 391 (1991).
56. C. Oseen, *Trans. Faraday Soc.* **29**, 883 (1933).
57. H. Zocher, *Trans. Faraday Soc.* **29**, 945 (1933).
58. F. C. Frank, *Discuss. Faraday Soc.* **25**, 19 (1958).
59. J. Nehring and A. Saupe, *J. Chem. Phys.* **54**, 337 (1971).
60. P. W. Anderson and W. F. Brinkman, in *The Helium Liquids,* eds. J. G. M. Armitage and I. E. Farquar (Academic Press, NY, 1975).

61. S. S. Rozhkov, *Usp. Fiz. Nauk* **148**, 325 (1986) [*Sov. Phys. Usp.* **29**, 186 (1986)].

62. L. Landau and E. M. Lifshits, *Electrodinamika Sploshnykh Sred,* 2nd ed. (Nauka, Moscow, 1982).

63. N. N. Bogoljubov and D. V. Shirkov, *Introduction to the Theory of Quantized Fields* (John Wiley. N. Y., 1980).

64. J. Nehring and A. Saupe, *J. Chem. Phys.* **56**, 5527 (1972).

65. G. Barbero, N. V. Madhusudana and C. Oldano, *J. Phys. (Paris)* **50**, 263 (1989).

66. P. I. C. Teixeira, V. M. Pergamenshchik and T. J. Sluckin, *Mol. Phys.* **80**, 1339 (1993).

67. R. D. Williams, *J. Phys.* **A19**, 3211 (1986).

68. S. Kralj and S. Zumer, *Phys. Rev.* **E45**, 2461 (1992).

69. P. Boltenhagen, O. D. Lavrentovich and M. Kléman, *J. Phys. II (France)* **1**, 1233 (1991).

70. P. Boltenhagen, O. D. Lavrentovich and M. Kléman, *Phys. Rev.* **A46**, 1743 (1992); P. Boltenhagen, M. Kléman and O. D. Lavrentovich, *C. R. Acad. Sci.* **315**, série II, 931 (1992).

71. V. M. Pergamenshchik, *Ukr. Fiz. Zh.* **35**, 1339 (1990).

72. G. Barbero, A. Sparavigna and A. Strigazzi, *Nuovo Cimento* **D12**, 1259 (1990).

73. V. M. Pergamenshchik, *Phys. Rev.* **E48**, 1254 (1993); *Phys. Rev.* **E49**, 934(E) (1994).

74. G. Barbero and R. Barberi, *J. Phys. (France)* **44**, 609 (1983).

75. S. Chandrasekhar, *Liquid Crystals* (Cambridge University Press, Cambridge, 1992).

76. H. Lee and M. M. Labes, *Mol. Cryst. Liq. Cryst. Lett.* **82**, 199 (1982).

77. N. V. Madhusudana and R. Pratibha, *Curr. Sci.* **51**, 877 (1982); *Mol. Cryst. Liq. Cryst.* **103**, 31 (1983).

78. Q.-F. Zhou, X.-H. Wan, F. Zhang, D. Zhang, Z. Wu and X. Feng, *Liq. Cryst.* **13**, 851 (1993).

79. G. E. Volovik, *Pis'ma Zh. Eksp. Teor. Fiz.* **28**, 65 (1978) [*JETP Lett.* **28**, 59 (1978)]; G. E. Volovik and O. D. Lavrentovich, *Zh. Eksp. Teor. Fiz.* **85**, 1997 (1983) [*Sov. Phys. JETP* **58**, 1159 (1983)].

80. N. D. Mermin, *Boojums All The Way Through* (Cambridge University Press, Cambridge, 1991), chap. 1.

81. I. Chuang, R. Durrer, N. Turok and B. Yurke, *Science* **251**, 1336 (1991).

82. E. Lonberg and R. Meyer, *Phys. Rev. Lett.* **55**, 718 (1985).

83. A. -M. Cazabat, *Mol. Cryst. Liq. Cryst.* **179**, 99 (1990).

84. B. Jérôme and M. Boix, *Phys. Rev.* **A45**, 5746 (1992).

85. R. Williams, *Phys. Rev. Lett.* **21**, 342 (1968); *J. Chem. Phys.* **50**, 1324 (1969).

86. D. Meyerhofer, A. Sussman, and R. Williams, *J. Appl. Phys.* **43**, 3685 (1972).

87. E. F. Carr, *Liq. Cryst.* **4**, 573 (1989).

88. R. B. Meyer, *Phys. Rev. Lett.* **22**, 918 (1969).

89. E. Dubois-Violette and O. Parodi, *J. Phys. (Paris)* Colloq. **30**, C4-57 (1969).

90. O. D. Lavrentovich, *Pis'ma Zh. Tekhn. Fiz.* **14**, 166 (1988) [*Sov. Tech. Phys. Lett.* **14** (1), 73 (1988)].

91. N. M. Golovataya, M. V. Kurik and O. D. Lavrentovich, *Liq. Cryst.* **7**, 287 (1990).

92. V. M. Bedanov, G. V. Gadiyak and Yu. E. Lozovik, *Phys. Lett.* **A92**, 400 (1982).

93. P. G. de Gennes, *C. R. Acad. Sci.,* Ser. **B271**, 469 (1970).

94. B. V. Deryagin, *Theory of the Stability of Colloids and Thin Films* (Nauka, Moscow, 1986).

95. R. G. Horn, J. N. Israelachvili and E. Perez, *J. Phys. (Paris)* **42**, 39 (1981).

96. J. P. Sethna and m. Kléman, *Phys. Rev.* **A26**, 3037 (1982).

97. P. E. Cladis and S. Torza, *J. Appl. Phys.* **46**, 584 (1975).

98. R. Bidaux, N. Boccara, G. Sarma, L. De Seze, P. G. de Gennes and O. Parodi, *J. Phys. (Paris)* **34**, 19 (1973).

99. O. D. Lavrentovich, *Zh. Eksp. Teor. Fiz.* **91**, 1661 (1986) [*Sov. Phys. JETP* **64**, 984 (1986)]; *Mol. Cryst. Liq. Cryst.* **151**, 417 (1987).

100. J. B. Fournier and G. Durand, *J. Phys. II France* **1**, 845 (1991).

101. Z. Li and O. D. Lavrentovich, *Phys. Rev. Lett.* **73**, 280 (1994), Z. Li, W. R. Folks, and O. D. Lavrentovich, *Inc. IS&T/SPIE Symposium on Electronic Imaging Science & Technology*, #2175-04, San Jose, CA (1994).

102. C. Oldano and G. Barbero, *J. Phys. Lett.* (Paris) **46**, L451 (1985); G. Barbero and C. Oldano, *Nuovo Cimento* **D6**, 479 (1985).

103. V. M. Pergamenshchik, *Ukr. Fiz. Zh.* **35**, 1218 (1990).

104. H. P. Hinov, *Mol. Cryst. Liq. Cryst.* **148**, 197 (1987).

105. H. P. Hinov, *Mol. Cryst. Liq. Cryst.* **168**, 7 (1987).

106. H. P. Hinov, *Mol. Cryst. Liq. Cryst.* **191**, 389 (1990).

107. H. P. Hinov, *Mol. Cryst. Liq. Cryst.* **209**, 339 (1990).

108. A. Rapini and M. Popoular, *J. Phys. Colloq.* (Paris) **30**, C4-54 (1969).

109. H. Mada, *Mol. Cryst. Liq. Cryst.* **51**, 43 (1979).

110. A. M. Samosa and P. Tarasona, *Mol. Phys.* **72**, 911 (1991).

111. T. J. Sluckin and A. Poniewierski, in *Fluid Interfacial Phenomena,* ed. C. A. Croxton (Wiley, New York, 1986).

112. A. K. Sen and D. E. Sullivan, *Phys. Rev.* **A35**, 1391 (1987).

113. M. Osipov, *Poverkhnost'* **9**, 39 (1988).

114. G. Barbero and A. Strigazzi, *J. Phys. Lett.* (Paris) **45**, 857 (1984).

115. N. V. Madhusudana and R. Pratibha, *Mol. Cryst. Liq. Cryst.* **179**, 207 (1990).

116. S. A. Pikin and E. M. Terent'ev, *Sov. Phys. Crystallogr.* **33**, 641 (1988).

117. S. Faetti, *Liq. Cryst.* **15**, 807 (1993).

118. S. Faetti, *Phys. Rev.* **E49**, 5332 (1994).

119. V. M. Pergamenshchik, *Ukr. Fiz. Zh.* **38**, 59 (1993).

120. V. M. Pergamenshchik, P. I. C. Teixeira and T. J. Sluckin, *Phys. Rev.* **E48**, 1265 (1993).

121. O. D. Lavrentovich and V. M. Pergamenshchik, *Phys. Rev. Lett.* **73**, 979 (1994).

122. A. L. Alexe-Ionescu, *J. Mod. Phys.* **B7**, 1131 (1993).

123. J. L. Eriksen, *Phys. Fluids* **99**, 1205 (1966).

124. Yu. A. Nastishin and O. D. Lavrentovich, unpublished results (1986).

125. E. Gorecka, private communication (1993).

126. R. B. Meyer and N. Clark, unpublished; see Ref. 131.

127. C. Allet, M. Kléman, and P. Vidal, *J. Phys. (Paris)* **39**, 181 (1978).

128. S. A. Langer and J. P. Sethna, *Phys. Rev.* **A34**, 5035 (1986).

129. A. E. Jacobs, G. Goldner, and D. Mukamel, *Phys. Rev.* **A45** 5783 (1992).

130. J. Ruiz-Garcia, X. Qui, M. -W. Tsao, G. Marshall, Ch. M. Knobler, G. A. Overbeck, and D. Mobius, *J. Phys. Chem.* **97**, 6955 (1993); D. K. Schwartz, J. Ruiz-Garcia, X. Qui, J. V. Selinger, and Ch. M. Knobler, *Physica* **A204**, 606 (1994).

131. R. Viswanathan, J. A. Zasadzinski, and D. K. Schwartz, *Nature* **368**, 440 (1994).

132. R. B. Meyer and P. S. Pershan, *Soild State Comm.* **13**, 989 (1973).

133. J. V. Selinger, *Mater. Res. Soc. Symp. Ser.* **248**, 29 (1992); J. V. Selinger and R. L. B. Selinger, submitted for publication (1994).

134. We thank T. C. Lubensky, R. G. Petschek, and J. Toner for the discussions of the correspondence between three- and two-dimensional elastic theories.